ORIGINAL RESEARCH

Abnormal Calcium Cycling and Cardiac Arrhythmias Associated With the Human Ser96Ala Genetic Variant of Histidine-Rich Calcium-Binding Protein

Vivek P. Singh, PhD; Jack Rubinstein, MD; Demetrios A. Arvanitis, PhD; Xiaoping Ren, MD; Xiaoqian Gao, BS; Kobra Haghighi, PhD; Mark Gilbert, MD; Venkat R. Iyer, MD; Do Han Kim, PhD; Chunghee Cho, PhD; Keith Jones, PhD; John N. Lorenz, PhD; Clara F. Armstrong, PhD; Hong-Sheng Wang, PhD; Sandor Gyorke, PhD; Evangelia G. Kranias, PhD

***Background*—**A human genetic variant (Ser96Ala) in the sarcoplasmic reticulum (SR) histidine-rich Ca^{2+}-binding (HRC) protein has been linked to ventricular arrhythmia and sudden death in dilated cardiomyopathy. However, the precise mechanisms affecting SR function and leading to arrhythmias remain elusive.

***Methods and Results*—**We generated transgenic mice with cardiac-specific expression of human Ala96 HRC or Ser96 HRC in the null background to assess function in absence of endogenous protein. Ala96 HRC decreased (25% to 30%) cardiomyocyte contractility and Ca^{2+} kinetics compared with Ser96 HRC in the absence of any structural or histological abnormalities. Furthermore, the frequency of Ca^{2+} waves was significantly higher (10-fold), although SR Ca^{2+} load was reduced (by 27%) in Ala96 HRC cells. The underlying mechanisms involved diminished interaction of Ala96 HRC with triadin, affecting ryanodine receptor (RyR) stability. Indeed, the open probability of RyR, assessed by use of ryanodine binding, was significantly increased. Accordingly, stress conditions (5 Hz plus isoproterenol) induced aftercontractions (65% in Ala96 versus 12% in Ser96) and delayed afterdepolarizations (70% in Ala96 versus 20% in Ser96). The increased SR Ca^{2+} leak was accompanied by hyperphosphorylation (1.6-fold) of RyR at Ser2814 by calmodulin-dependent protein kinase II. Accordingly, inclusion of the calmodulin-dependent protein kinase II inhibitor KN93 prevented Ser2814 phosphorylation and partially reversed the increases in Ca^{2+} spark frequency and wave production. Parallel in vivo studies revealed ventricular ectopy on short-term isoproterenol challenge and increased (4-fold) propensity to arrhythmias, including nonsustained ventricular tachycardia, after myocardial infarction in Ala96 HRC mice.

***Conclusions*—**These findings suggest that aberrant SR Ca^{2+} release and increased susceptibility to delayed afterdepolarizations underlie triggered arrhythmic activity in human Ala96 HRC carriers. **(*J Am Heart Assoc*. 2013;2:e000460 doi: 10.1161/JAHA.113.000460)**

Key Words: arrhythmia • calcium • ryanodine receptor calcium release channel • sarcoplasmic reticulum

From the Departments of Pharmacology and Cell Biophysics (V.P.S., X.R., X.G., K.H., K.J., H.-S.W., E.G.K), Medicine (J.R., M.G), and Physiology (J.N.L), University of Cincinnati College of Medicine, Cincinnati, OH; Biomedical Research Foundation, Athens, Greece (D.A.A, E.G.K.); Gwangju Institute of Science and Technology, Gwangju, Korea (D.H.K., C.C); University of Pennsylvania, Philadelphia (C.F.A); Children's Hospital Philadelphia, Philadelphia (V.R.I); Davis Heart and Lung Research Institute, Ohio State University, Columbus, OH (S.G).

Accompanying Tables S1 and S2, Figures S1 through S3 are available at http://jaha.ahajournals.org/conten/2/5/e000460/suppl/DC1

Correspondence to: Evangelia G. Kranias, PhD, Department of Pharmacology and Cell Biophysics, University of Cincinnati College of Medicine, 231 Albert Sabin Way, Cincinnati, OH 45267-0575. E-mail: Litsa.Kranias@uc.edu

Received August 1, 2013; accepted September 12, 2013.

Dilated cardiomyopathy (DCM) is associated with a high incidence of ventricular arrhythmias and increased risk of sudden cardiac death from ventricular tachycardia (VT) and ventricular fibrillation.[1,2] The underlying etiologies are not well defined, but impaired Ca^{2+} cycling and increased diastolic sarcoplasmic reticulum (SR) Ca^{2+} leak via ryanodine receptor 2 (RyR2) have been implicated as a major etiology in the induction of delayed afterdepolarizations (DADs) leading to deleterious ventricular arrhythmias.[3,4] This defect has been linked to abnormal regulation of RyR2 by luminal Ca^{2+} and regulatory proteins,[5,6] suggesting that targeting these molecules may constitute potential therapy for the treatment of heart failure and malignant arrhythmias.

In this regard, the histidine rich Ca^{2+}-binding protein (HRC) has recently emerged as a key regulator of SR Ca^{2+} cycling.[7–10] HRC regulates SR Ca^{2+} uptake through a direct interaction

with sarcoplasmic reticulum Ca^{2+} ATPase 2a and inhibits cardiomyocyte relaxation.[10] In addition, HRC binds to triadin,[11,12] a member of the SR Ca^{2+} release channel complex,[13] suggesting that HRC may also regulate RyR2 function. The functional importance of HRC is highlighted by the identification of a human genetic variant (Ser96Ala) that was linked to life-threatening ventricular arrhythmias and sudden death in a well-characterized cohort of patients with idiopathic DCM.[14] Furthermore, the percentage of homozygous Ala/Ala patients with an implantable cardioverter-defibrillator was almost double that of the Ser/Ala heterozygotes, suggesting a strong dosage effect of this HRC genetic variant on ventricular arrhythmias. Indeed, acute overexpression of the human Ala96 HRC variant in isolated adult rat cardiomyocytes by adenoviral gene transfer resulted in aberrant Ca^{2+} transient kinetics and increased frequency of Ca^{2+} sparks.[15]

Previous genetic studies have confirmed the role of defective cardiomyocyte Ca^{2+} handling in the pathogenesis of various inherited arrhythmic syndromes. Support for this notion has been provided by the identification and characterization of human mutations in the *RyR2*, calsequestrin 2 (*CASQ2*), and triadin genes, which have been linked to catecholaminergic polymorphic ventricular tachycardia, leading to syncope and sudden cardiac death. The underlying mechanisms involve impaired activity or regulation of the RyR2 channel.[16–19]

The present study addressed the in vivo pathophysiological mechanisms associated with the human HRC variant, which was shown to correlate with life-threatening ventricular arrhythmias in DCM.[14] We chose to express the human HRC, which is considerably different than mouse HRC,[20] in the heart of the null (HRC-KO) background,[8] to examine its function in the absence of the endogenous mouse protein. Here, we demonstrate that Ala96 HRC altered intracellular Ca^{2+} handling and promoted arrhythmogenic events in vitro and in vivo, indicating that this variant serves as a susceptibility factor to life-threatening arrhythmias in DCM carriers.

Methods

Generation and Identification of Transgenic Mice Expressing Human HRC

An expression construct was generated containing the cardiac-specific α-myosin heavy chain promoter (α-MHC_P, 5.5 kb; a gift from J. Robbins, Children's Hospital, Cincinnati, OH), the human HRC cDNA with the HRC Ser96 or HRC Ala96 mutation (HRC cDNA, 3.94 kb; introduced via PCR), and the human growth hormone polyadenylation signal. Microinjection and identification of transgenic mice were performed as described previously.[9] Transgenic C57/BL6 mice with cardiac-specific expression of the human HRC cDNA carrying either the human *Ser96 HRC* or *Ala96 HRC* were mated with the HRC-KO mice (C57/BL6) (HRC-KO model was obtained from Dr Do Han Kim, Gwangju Institute of Science and Technology [GIST], Gwangju, Republic of Korea).[8] F_1 heterozygous HRC offspring with the HRC mutant transgenes were identified by using PCR methodology and bred with HRC-KO mice to obtain the F_2 generation. The HRC-KO offspring carrying the human HRC variant transgenes were selected to backcross with HRC-KO mice for at least 3 generations before using them for our studies. The handling and maintenance of animals were approved by the ethics committee of the University of Cincinnati. Eight- to 12-week-old mice were used for all studies. The investigation conformed to the "Guide for the Care and Use of Laboratory Animals" of the National Institutes of Health.

Mouse Myocyte Isolation and Measurements of Mechanics and Ca^{2+} Kinetics

Isolation of mouse left ventricular myocytes was carried out as described previously.[21] Briefly, mouse hearts were excised from anesthetized (pentobarbital sodium 70 mg/kg IP) adult mice, mounted in a Langendorff perfusion apparatus, and perfused with Ca^{2+}-free Tyrode's solution at 37°C for 3 minutes. The normal Tyrode's solution contained (in mmol/L) NaCl 140, KCl 4, $MgCl_2$ 1, glucose 10, and HEPES 5, pH 7.4. Perfusion was then switched to the same solution containing 75 units/mL type 1 collagenase (Worthington), and perfusion continued until the heart became flaccid (≈10 to 15 minutes). The left ventricular tissue was excised, minced, pipette-dissociated, and filtered through a 240-μm screen. The cell suspension was then sequentially washed in 25, 100, and 200 μmol/L and 1 mmol/L Ca^{2+}-Tyrode's and resuspended in 1.8 mmol/L Ca^{2+}-Tyrode's for further analysis. To obtain intracellular Ca^{2+} signals, cells were incubated with the acetoxymethyl ester form of fura-2 (Fura-2/AM; 2 μmol/L) for 30 minutes and resuspended in 1.8 mmol/L Ca^{2+}-Tyrode's solution. The myocyte suspension was placed in a Plexiglas chamber, which was positioned on the stage of an inverted epifluorescence microscope (Nikon Diaphot 200), and perfused with 1.8 mmol/L Ca^{2+}-Tyrode's solution. Cell shortening and Ca^{2+} transients were measured at room temperature (22° to 23°C) in separate experiments, as documented here later. The room temperature allowed the myocytes to be stable for up to 2 hours with constant pacing. Myocytes were field stimulated to contract by using a Grass S5 stimulator through platinum electrodes placed alongside the bath (0.5 Hz, bipolar pulses with voltages 50% above myocyte voltage threshold). Contractions of myocytes from random fields were videotaped and digitized on a computer. For Ca^{2+} signal measurements, cells were loaded with Fura-2/AM 2 μmol/L and alternately excited at 340 and 380 nm by a use of a Delta Scan dual-beam spectrophotofluorometer

(Photon Technology International) at baseline conditions and on 100 nmol/L isoproterenol (ISO) stimulation. Ca^{2+} transients were expressed as the 340/380 nm ratios of the resulting 510-nm emissions. Rapid application of 10 mmol/L caffeine was used to induce release of SR Ca^{2+} and to assess SR Ca^{2+} load. Cells were superfused with normal Tyrode's solution and stimulated at 0.5 Hz until twitch characteristics stabilized before each caffeine application. The caffeine solution was introduced into the chamber via a quick switching device and was present during the study (30 seconds) of the kinetics of $[Ca]_i$ decline.[22] The amplitude of the caffeine-induced Ca^{2+} transients can be used as an index of SR Ca^{2+} content. Decline of $[Ca]_i$ during a caffeine-induced Ca^{2+} transient in normal Tyrode's was attributable to Na-Ca exchange. Measurements of mechanics and Ca^{2+} kinetics were also performed in the presence of 100 nmol/L ISO at 0.5 Hz. Data were analyzed by the use of Felix software (Photon Technology International).

Quantitative Immunoblotting

Alterations in the levels of total proteins or their phosphorylation status were analyzed from whole heart homogenates through Western blotting. For phosphoproteins, hearts were retrogradely perfused through the aorta with Tyrode's solution at constant flow at 37°C for 2 minutes to wash out blood. Perfusion was then continued with Tyrode's solution with or without 100 nmol/L ISO for 5 minutes before rapid freezing. The Tyrode's solution was supplemented with 20 mmol/L NaF, 0.005 mmol/L okadaic acids, to keep the phosphorylation status of the proteins. Briefly, an appropriate amount of heart homogenate was separated via SDS-PAGE (4% to 12%) and transferred to a nitrocellulose membrane (Bio-Rad). After blocking with 5% nonfat milk, membranes were incubated with primary antibodies, followed by appropriate secondary antibodies. Primary antibodies against various proteins of interest used in this study were as follows: pSer16-PLN, pThr17-PLN, pSer2808-RyR2, and pSer2814-RyR2 (Badrilla), PLN (Upstate Biotechnology), RyR2 (Sigma Aldrich), SR Ca^{2+} ATPase 2a, sodium calcium exchanger (NCX), triadin, and GAPDH (Affinity Bioreagents). The horseradish peroxidase–conjugated anti-mouse or antirabbit secondary antibodies (1:5000) were from Amersham Biosciences. The membranes were developed by using an enhanced chemiluminescence Western blot analysis detection system (Amersham Biosciences). All the protein levels were quantified using AlphaEaseFC software (Alpha Innotech).

Ca^{2+} Overlay Assay

Enriched SR membrane fractions were isolated from Ser96 and Ala96 hearts, and different amounts (25, 50, and 100 μg) of protein were analyzed by using SDS-PAGE. The proteins were transferred to nitrocellulose membranes, and the Ponceau red stain was then washed off the nitrocellulose membrane with TBS buffer. The membrane was incubated in (in mmol/L) imidazole 10, pH 6.8, KCl 60, and $MgCl_2$ 5. Thereafter, the membrane was incubated with 1 μCi of $^{45}Ca^{2+}$/mL supplemented with 1 mmol/L $CaCl_2$ at room temperature for 20 minutes, as described previously.[23,24] The membrane was rinsed with dH_20 and analyzed by use of a Storm 860.

Stains-all Staining

Stains-all is a cationic carbo-cyanine dye that stains Ca^{2+}-binding proteins blue or red depending on the conditions.[25] Briefly, 5 to 15 μg of whole heart homogenates from wild-type (WT) (nontransgenic), Ser96 and Ala96 mice were separated via 8% SDS-PAGE, and the gels were washed with 25% isopropanol to remove SDS (5×20 minutes). The gel was then fixed overnight with 25% isopropanol. Thereafter, the gel was exposed to Stains-all solution (0.025% Stains-all [ACROS Organics], 7.5% formamide, 25% isopropanol, 30 mmol/L Tris base, pH 8.8) for 48 hours in a container protected from light. Following staining, the gel was washed extensively overnight in 25% isopropanol to destain. Stains-all stained gels were photographed with a Gel Doc EZ system (Bio-Rad).

Induction of Aftercontractions and DADs in Isolated Cardiomyocytes

Rod-shaped ventricular myocytes, which exhibited no spontaneous activity at rest, were paced at 5 Hz in the presence of 1 μmol/L ISO in 1.8 mmol/L Ca^{2+}-Tyrode's solution at room temperature. After 2 or 3 trains of stimulation, pacing was stopped to allow the recording of spontaneous aftercontractions within 2 to 5 seconds. For electrophysiology recordings, isolated ventricular myocytes were perfused with Tyrode's solution containing (in mmol/L): NaCl 140, KCl 5.4, $MgCl_2$ 1, $CaCl_2$ 1.8, HEPES 5, and glucose 10, pH 7.4. Whole-cell patch-clamp recordings were used to determine action potential. Glass pipettes were filled with a solution containing (in mmol/L) K-aspartate 110, KCl 20, EGTA 10, HEPES 10, $MgCl_2$ 2.5, NaCl 8, $CaCl_2$ 1, Na_2-ATP 2, and Na-GTP 0.1, pH adjusted to 7.2 with KOH, and had a resistance of 1.5 to 2.0 mol/L. Action potentials were recorded under current-clamp mode and triggered by 2-ms just-threshold current steps at a frequency of 5 Hz in the presence of 1 μmol/L ISO at 35°C. Stimulation was then withdrawn to determine the presence of DADs as described previously.[26] Whole-cell patch-clamp recordings were performed with an Axopatch-1B amplifier. Data were collected using PCLAMP9 software through an Axon Digidata 1322A data acquisition system. All chemical and drugs were from Sigma unless otherwise stated.

Measurement of Ca^{2+} Sparks and Waves

Ca^{2+} sparks were recorded in intact myocytes loaded with fluo-4 AM (10 μmol/L; Molecular Probes) for 15 minutes at room temperature and then washed with Tyrode's solution. Myocytes were superfused with normal Tyrode's solution (1.8 mmol/L $CaCl_2$) or the same solution containing 100 nmol/L ISO, in a custom-made glass-plexiglass recording chamber at room temperature (24°C). Spontaneous Ca^{2+} sparks were obtained in quiescent cells after 0.5-Hz stimulation (for 1 minute) to reach steady state and to ensure equal SR Ca^{2+} load. Fluorescence images were recorded using a Zeiss LSM 510 inverted confocal microscope through a ×40 water-immersion objective lens with excitation wavelength of 488 nm. Fluorescence signals were measured at greater than 515 nm with line-scan imaging at 3.07-ms intervals, with each line comprising 512 pixels spaced at 0.056 μm. In the presence of 1 μmol/L ISO and after 2 trains of 5-Hz stimulation, Ca^{2+} waves were recorded using similar methods as Ca^{2+} sparks. Ca^{2+} spark amplitude was normalized as F/F_0, duration was taken from the full-duration half-maximum, and width was taken from full-width half-maximum. In some experiments, myocytes were incubated with the calmodulin-dependent protein kinase II inhibitor (1 μmol/L KN-93 [Sigma]) for 15 minutes, and Ca^{2+} sparks were then measured in the absence or presence of ISO. Image processing and data analysis were performed using IDL software (ITT Visual Information Solutions).[27]

ISO-Induced Arrhythmias

Mice were anesthetized using 2.5% Avertin and an equivalent of lead I ECG recording (PowerLab; AD Instruments) was performed as previously described.[26] After stabilization of the preparation, a control ECG was recorded for 5 minutes. This was followed by an intraperitoneal injection of ISO 2 mg/kg body weight (Sigma) and a subsequent recording period of 20 minutes. During this period, ECGs were analyzed for ISO-induced arrhythmias.

Myocardial Ischemia/Reperfusion In Vivo

In vivo myocardial ischemia/reperfusion (I/R) was performed through ligation of the left anterior descending coronary artery (LAD) and release of the ligature, as previously described.[28] The LAD was ligated at 2 mm distal from the tip of the left appendix for a period of 30 minutes, and this was followed by releasing the ligation and closing the chest. Ischemia was confirmed by visual observation (cyanosis) and continuous ECG monitoring, using electrodes placed subcutaneously to record data by the PowerLab system (Australia AD Instruments). At different time points after myocardial infarction (MI), mice were anesthetized with 1.0% to 1.5% isoflurane in O_2 and placed on a heating pad (37°C), and cardiac function was assessed by echocardiography, using a Visualsonic Vevo 770 ultrasound equipped with a 30-MHz transducer applied to the chest wall. Cardiac ventricular dimensions and ejection fraction (EF) were assessed in 2-dimensional mode. Analyses were performed by observers blinded to the genotype of the animals. To monitor ventricular arrhythmias and sudden death after I/R, radio transmitters (EA-F20; Data Science International) for ECG recording were implanted in mice 1 week before MI surgery, and ECGs were recorded continuously for 12 weeks after MI.

Coimmunoprecipitation Studies

HEK 293 cells (ECACC) were maintained in Dulbecco's modified Eagle's medium supplemented with 10% fetal bovine serum (Invitrogen). Full-length green fluorescent protein (GFP)-rabbit triadin (GenBank: U31540.1, producing a protein of ≈60 kDa with the tag) and GFP-hHRC Ser96 or GFP-hHRC Ala96 constructs (of approximate size 157 kDa with the tag) were transiently transfected in HEK 293 cells with Lipofectamine 2000 (Invitrogen), according to the manufacturer's instructions. Forty-eight hours after transfection, cells were harvested and lysed in 50 mmol/L Tris-HCl, 150 mmol/L NaCl, 1% NP40 with protease inhibitors. Cell lysates were precleared with 30 μL of protein G–Sepharose (Amersham Biosciences Europe) for 1 hour at 4°C. The precleared cell lysates were then incubated with 4 μg of HRC (Sigma-Aldrich) antibody and 30 μL of protein G–Sepharose at 4°C overnight. The beads were washed 3 times with lysis buffer and were analysed by western blot with human anti-HRC (Sigma-Aldrich) or anti-GFP (Sigma-Aldrich) antibodies. Co-immunoprecipitation was also performed using anti-HRC antibody and cardiac homogenates (1 mg total protein) of Ser96 and Ala96 HRC mice.[29] The precipitates were analyzed by immunoblotting with anti-HRC and anti-Triadin (TRD) antibodies, as indicated. Immunoprecipitate with anti-IgG PLUS agarose was used as negative control.

Electron Microscopy

Hearts were fixed by perfusion through the left ventricle with 3.5% glutaraldehyde in 0.1 mol/L sodium cacodylate buffer, pH 7.2. Papillary muscles were excised, rinsed in 0.1 mol/L cacodylate buffer, postfixed in buffered 2% OsO_4 for 1 hour at 4°C, rinsed in H_2O, en bloc stained with saturated uranyl acetate, and embedded in epon. Thin sections were examined with use of a Philips 410 electron microscope (Philips Electron Optics), and the images recorded digitally with a Hamamatsu C4742-95 digital camera (Advanced Microscopy Techniques).[30]

Measurement of Diastolic SR Ca^{2+} Leak

Diastolic SR Ca^{2+} leak was measured using the protocol described previously.[30] Fura-2–loaded cardiac myocytes were field stimulated at 1 Hz until they reached a steady-state Ca^{2+} transient height. Stimulation was then switched off, and the external solution was quickly changed to Tyrode's solution $0Ca^{2+}$, $0Na^{+}$ to eliminate transsarcolemmal Ca^{2+} fluxes, resulting in a new steady state $[Ca^{2+}]_i$. When RyR2 channels are inhibited by 1 mmol/L tetracaine (in Tyrode's solution, $0Ca^{2+}$, $0Na^{+}$), Ca^{2+} shifts from the cytosol into the SR. The tetracaine-induced drop in diastolic Fura-2 fluorescence ratio was used as an estimate of SR Ca^{2+} leak, which is insensitive to changes in SR Ca^{2+} uptake. Then, the myocytes were exposed for 4 seconds to $0Ca^{2+}$, $0Na^{+}$ Tyrode's solution containing 10 mmol/L caffeine and 20 mmol/L 2,3-butanedione monoxime (to prevent myocyte hypercontracture). The amplitude of caffeine-induced Ca^{2+} transient was used as an estimate of total $[Ca^{2+}]_i$, which included the Ca^{2+} leak.

Preparation of Mouse Crude Membrane Fractions and [^{3}H]Ryanodine Binding

Mouse hearts were perfused for 5 minutes with Ca^{2+}-free Tyrode's solution (pH 7.4) complemented with 20 mmol/L NaF^{+} and 0.005 mmol/L okadaic acid. Hearts were then frozen in liquid nitrogen and crushed into fine powder. The powder was suspended in 1 mL of ice-cold sucrose buffer (0.3 mol/L sucrose, 20 mmol/L HEPES, 20 mmol/L NaF, pH 7.2 with KOH) containing protease inhibitors (12 mmol/L leupeptin, 100 mmol/L phenylmethylsulfonyl fluoride, 500 mmol/L benzamidine, and 1 mg/mL aprotinin) and homogenized on ice. The total homogenate was centrifuged at 42 000*g* for 45 minutes at 4°C. The 42 000*g* pellet (crude membrane fraction) was resuspended in the same sucrose buffer described earlier, aliquoted, quickly frozen, and stored at −80°C before use. Protein concentrations were determined by use of the Bradford method. [^{3}H]Ryanodine-binding experiments were performed with crude membrane fractions from individual hearts as described by El-Hayek and cols.[31] The incubation medium contained 150 nmol/L KCl, 20 mmol/L HEPES, pH 7.2 with KOH, 56 μg of cardiac membrane fraction, 10 nmol/L [^{3}H] ryanodine, and 1 mmol/L $CaCl_2$ (total volume 1000 μL). All incubations lasted 60 minutes at 37°C. Samples were run in duplicate, filtered onto glass fiber filters (Whatman GF/B), and washed 3 times with 5 mL of cold water using a Brandel M-24R cell harvester. The filters were placed in scintillation vials, 8 mL of liquid scintillation mixture was added, and the retained radioactivity was measured in a Beckman LS-3801 β-counter. The specific binding was defined as the difference between the binding in the absence (total binding) and presence (nonspecific binding) of 20 μmol/L unlabeled ryanodine. Fitting of data was accomplished with the computer program Origin (version 7.5, Microcal Inc).

Histology and Immunocytochemistry

Hearts of 8- to 10-week-old mice (Ser96 HRC, n=3; Ala96 HRC, n=3) were excised, stored in 10% formalin, and serially sectioned. The presence of macroscopic alterations of the heart was assessed by gross inspection; the heart was weighed to determine the heart/body weight ratio. Sections were stained with hematoxylin-eosin and Mason stain and evaluated by light microscopy. Isolated ventricular myocytes were processed using an established protocol.[32] Coverslips were incubated with polyclonal human anti-HRC (Sigma Aldrich) and monoclonal anti-SR Ca^{2+} ATPase (Affinity bioreagents) antibodies. After washing, cells were incubated with secondary antibodies (Alexa Fluor antirabbit 594 or Alexa Fluor antimouse 488, Invitrogen) with 1:500 (vol/vol) dilution in blocking buffer. Immunofluorescence images were generated from serial sections of isolated cardiomyocytes using Zeiss confocal microscopy.

Statistical Analysis

Data were expressed as mean±SEM. Comparisons between the means of 2 groups were performed by unpaired Student's *t* test. For multiple-groups comparisons, 1-way ANOVA was followed by post-hoc Newman-Keuls tests. Quantitative analysis of protein expression and phosphorylation levels were compared using a 1- or 2-way ANOVA and post-hoc Newman-Keuls tests. A repeated-measures 2-way ANOVA test was followed by a Bonferroni post hoc test to examine the effect of drug application (before versus after) between multiple groups. For the studies on isolated cardiomyocytes, 5 to 12 cells per heart were analyzed. The number of hearts/group (N=3 to 5 hearts per group) is indicated. Data from multiple myocytes (n=5 to 12 myocytes/heart) was averaged and the group means were then compared (Ser96 versus Ala96) using ANOVA/*t* test, wherever applicable. The Mann–Whitney *U* test was used to compare absolute premature ventricular complex incidence and Fisher exact test was used to evaluate ventricular tachycardia incidence. Categorical data were expressed as percentages and were compared with use of the Fisher exact test. Values of $P<0.05$ were considered significant.

Results

Cardiac Expression of Human Ser96 HRC and Ala96 HRC in the Null Background

We generated mice with cardiac-specific expression of the human Ser96 or Ala96 HRC variant in the HRC-KO

background to determine their effects in the absence of endogenous mouse HRC. This approach was chosen since there is only 48% amino acid homology between human and mouse.[20] We obtained several lines and chose 2 with similar levels of Ser96 and Ala96 HRC expression as those observed in mouse WT heart for further characterization studies (Figure S1). Cardiac expression of human Ser96 or Ala96 HRC did not elicit any alterations in Ca^{2+}-cycling protein levels, compared with WT hearts (Figure 1A and 1B). Importantly, the triadin levels, which were previously shown to increase on over-expression of HRC,[9,15] remained unaltered. This may be due to the controlled HRC expression in transgenic hearts since its levels were similar to WT levels (Figure S1). Histological and electron microscopy examination of papillary muscles revealed normal cardiac structure, and both Ser96 and Ala96 HRC co-localized with SR Ca^{2+} ATPase at the Z-line (Figure 1C and 1D).

Decreased Contractility and Ca^{2+} Transient Kinetics in Ala96 HRC Cardiomyocytes

HRC is an SR intraluminal Ca^{2+}-binding protein that regulates cardiac excitation–contraction coupling. To elucidate the role of the Ala96 HRC variant on SR Ca^{2+} cycling, we then examined isolated cardiomyocyte mechanics and Ca^{2+} kinetics from mice expressing the human Ser96 or Ala96 HRC. Ala96 cells exhibited decreases in fractional shortening (25%) and rates of contraction (23%) and relaxation (25%),

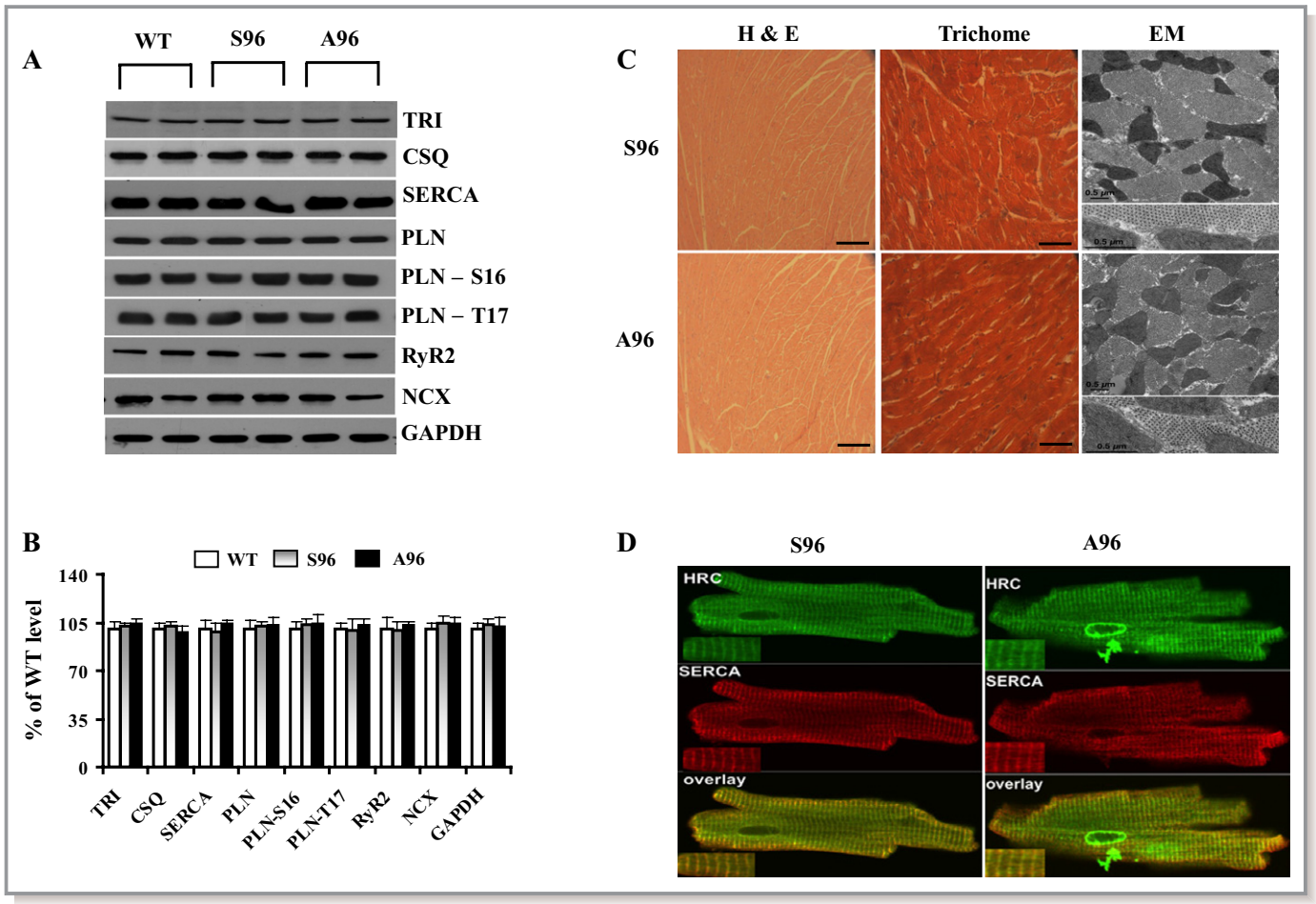

Figure 1. SR Ca^{2+}-cycling proteins and gross inspection of Ser96 (S96) and Ala96 (A96) HRC hearts. A, Representative blots of Ca^{2+}-cycling protein levels in WT (nontransgenic), Ser96, and Ala96 HRC hearts. B, Quantitative assessment of protein levels in WT (nontransgenic), Ser96, and Ala96 HRC hearts. Values are mean±SEM; N=3 hearts/group. C, Left: hematoxylin-eosin staining of ventricular sections of Ser96 and Ala96 HRC mice (×100), bars=10 μm. Middle: trichromic Masson stain of ventricular sections of Ser96 and Ala96 HRC (×100), bars=10 μm. Right: representative electron micrographs (EM) from cross sections of the papillary muscles from Ser96 and Ala96 HRC hearts. D, Ventricular cardiomyocytes from Ser96 and Ala96 mice immunostained with human anti-HRC and mouse anti-SERCA antibodies. Bars=20 μm. CSQ indicates calsequestrin; GAPDH, glyceraldehydes 3-phosphate dehydrogenase; HRC, histidine-rich Ca^{2+}-binding protein; NCX, sodium-calcium exchanger; PLN, phospholamban; PLN-16 and PLN-17, PLN phosphorylation at Ser16 and Thr17 sites; RyR2, ryanodine receptor; SERCA, sarcoplasmic reticulum Ca^{2+} ATPase; SR, sarcoplasmic reticulum; TRI, triadin; WT, wild type.

compared with the values in Ser96 cells (Figure 2A through 2D). Consistent with the contractile parameters, analysis of Ca^{2+} transients demonstrated that the Ca^{2+} amplitude (Fura-2 ratio, 340/380 nm), measured by peak changes from baseline, was decreased by 36% in Ala96 myocytes (Figure 2E and 2F). Furthermore, T_{80} (time to 80% decay of calcium peak) and τ were prolonged by ≈30% in Ala96 cells, compared with Ser96 (Figure 2G and 2H). Thus, the impairment in cellular contractility was associated with attenuated cytosolic Ca^{2+}-cycling kinetics in Ala96 myocytes. To examine the effects of β-adrenergic agonists, isolated cardiomyocytes were subjected to maximal ISO (100 nmol/L) stimulation and the contractile parameters and Ca^{2+} kinetics were evaluated. ISO stimulation resulted in enhancement of contractile parameters, including ±dL/dt and fractional shortening in both Ser96 and Ala96 myocytes, and the maximally stimulated parameters were similar between the 2 groups (Figure 2B through 2D). Similarly, Ca^{2+} transient amplitude, T_{80}, and τ were significantly stimulated in both groups, and the maximally stimulated parameters were not different between Ser96 and Ala96 cardiomyocytes (Figure 2F through 2H).

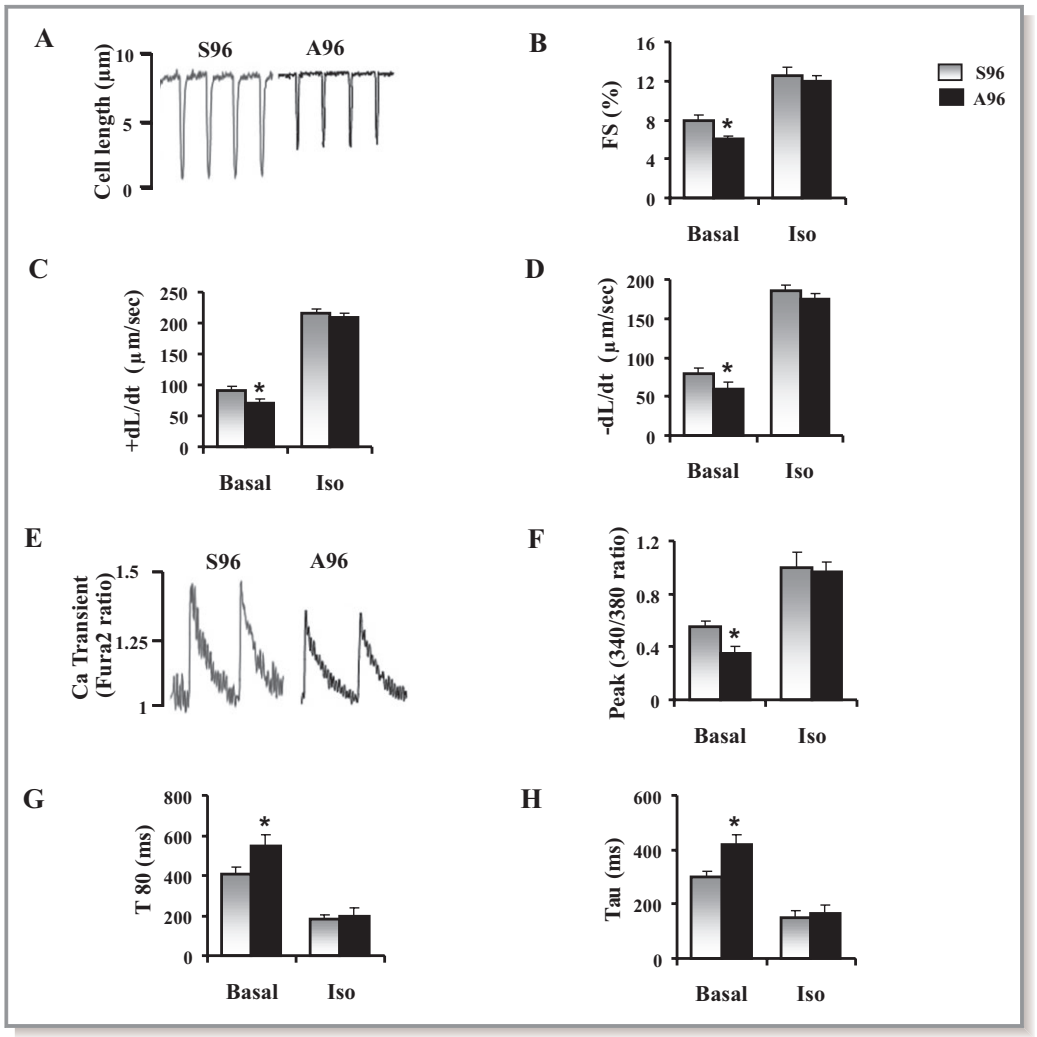

Figure 2. Mechanics and Ca^{2+} kinetics of Ser96 (S96) and Ala96 (A96) HRC myocytes and their responses to isoproterenol. A, Representative cell shortening tracings of Ser96 and Ala96 cells before isoproterenol stimulation, field stimulated at 0.5 Hz. B, The fractional shortening (FS) in the absence and presence of 100 nmol/L isoproterenol (ISO). C, Rates of contraction, +dL/dt, in the absence and presence of ISO. D, Rates of relaxation, −dL/dt, in the absence and presence of ISO. E, Representative tracings of Ca^{2+} transients in Ser96 and Ala96 cells before isoproterenol stimulation. F, Ca^{2+} transient amplitude, as indicated by the Fura-2 ratio (340:380 nm) in the absence and presence of ISO. G, Time to 80% decay of the transient (T80) in the absence and presence of ISO. H, Ca^{2+} transient decline (Tau). For cell mechanics (−ISO): n=44 to 55 cells from 5 hearts/group; twitch Ca^{2+} transients (−ISO): n=40 to 55 cells from 5 hearts/group; cell mechanics (+ISO): n=25 to 35 cells from 4 hearts/group, and Ca^{2+} transients (+ISO): n=38 to 50 cells from 3 hearts/group. Data are mean±SEM of the total number of cells/group. Comparisons were performed by using *t* test. *$P \leq 0.05$ vs Ser96 mice. HRC indicates histidine-rich Ca^{2+}-binding protein.

Reduced SR Ca^{2+} Content but Unchanged NCX Activity

Since the Ca^{2+} transient amplitude depends on SR Ca^{2+} load, we next measured SR Ca^{2+} content in ventricular myocytes (Figure 3A). As summarized in Figure 3B, the amplitude of caffeine-induced Ca^{2+} release was decreased by 27%, which indicates lower SR Ca^{2+} content in Ala96 cells under basal conditions. These results suggest that a decrease in SR Ca^{2+} load accounts for the reduction in systolic $[Ca^{2+}]_i$ transients and the associated lower contraction observed in Ala96 myocytes. NCX function, assessed as the time constant (τ) of Ca^{2+} decline during caffeine-induced Ca^{2+} transients,[22] indicated no difference in Ala96 versus Ser96 cardiomyocytes (Figure 3C). We then evaluated the effects of ISO on SR Ca^{2+} content. ISO increased Ca^{2+} load in both Ser96 and Ala96 cells but the levels were still lower in the Ala96 myocytes (Figure 3B). To determine how much Ca^{2+} is released at each twitch with respect to the total amount of Ca^{2+} stored, we evaluated the fractional release by normalizing the electrically evoked $[Ca^{2+}]_i$ transient to the caffeine-evoked $[Ca^{2+}]_i$ transient in each cell tested. Although fractional release was not different between the 2 groups at baseline (absence of ISO), it was significantly higher in Ala96 than Ser96 cells, following ISO stimulation (Figure 3D).

Increased Ca^{2+} Sparks and Waves in Ala96 Myocytes

At the myocyte level, heart failure or RyR2 mutations enhance SR Ca^{2+} leak, manifested as increases in Ca^{2+} sparks or waves, and this serves as the molecular trigger for arrhythmia.[33] To determine the effect of Ala96 on SR Ca^{2+} release, we examined Ca^{2+} spark properties with or without 100 nmol/L ISO stimulation in intact quiescent cells. The line-scan images and mean data for Ca^{2+} sparks in the presence of ISO are presented in Figure 4A. In the absence or presence of ISO, spark frequency was significantly higher in Ala96 cardiomyocytes with respect

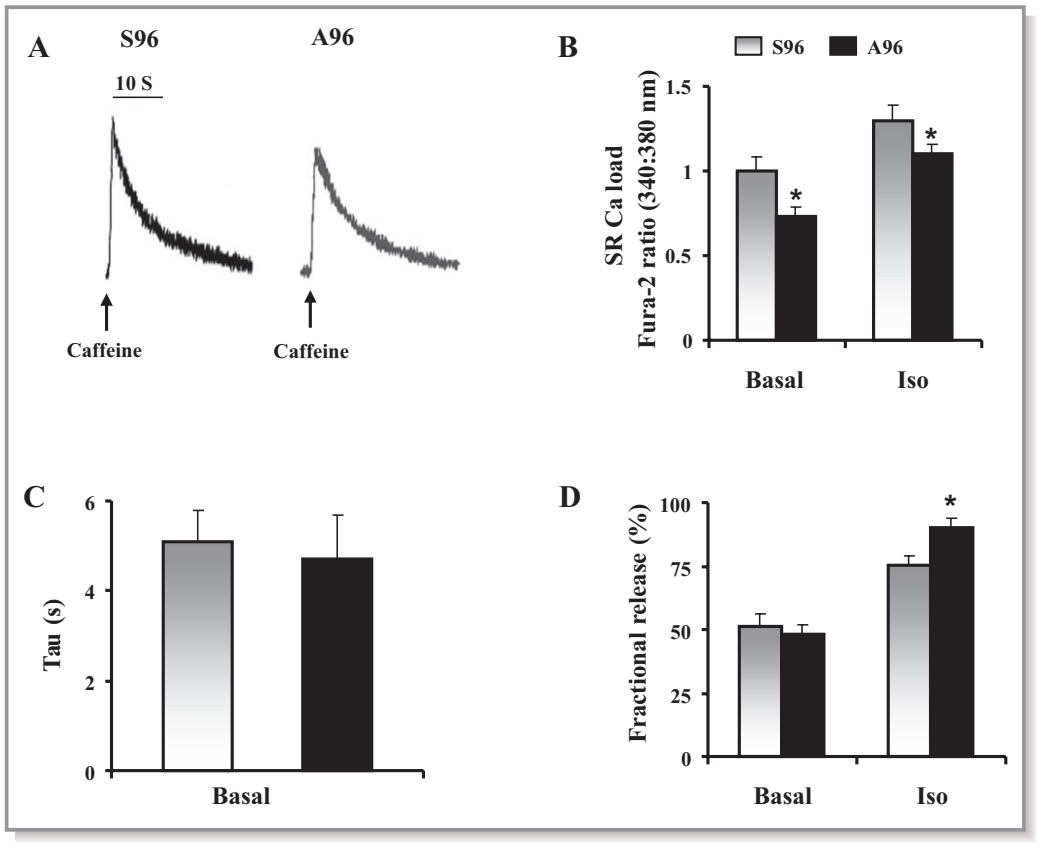

Figure 3. SR Ca^{2+} content and NCX function in Ser96 (S96) and Ala96 (A96) HRC cardiomyocytes. A, Representative tracings of caffeine-induced Ca^{2+} transients recorded from Fura-2 AM–loaded, field-stimulated myocytes at 0.5 Hz. B, Amplitude of caffeine-induced Ca^{2+} transients showing a decrease in SR Ca^{2+} load in myocytes from Ala96 mice in the absence and presence of ISO. C, Mean data for Ca^{2+} transient decline (Tau) during caffeine-induced Ca^{2+} transients, recorded in the presence of caffeine. D, Average data for fractional release (ratio of twitch Ca^{2+} transient/caffeine-induced Ca^{2+} transient). ISO (100 nmol/L). For SR Ca^{2+} load, n=15 to 25 cells for 4 Ser96 hearts; n=25 to 38 cells from 4 Ala96 hearts. Data are represented as mean±SEM of the total number of cells/group, and t test was used to calculate statistical significance. *P<0.05 vs Ser96 mice. AM indicates acetoxymethyl; HRC, histidine-rich Ca^{2+} binding; ISO, isoproterenol; NCX, sodium-calcium exchanger; SEM, standard error of the mean; SR, sarcoplasmic reticulum.

to Ser96 cardiomyocytes (Figure 4A and 4B and Table S1). Furthermore, spark amplitude, full width at half maximal amplitude, and full duration at half maximal amplitude were unchanged in the absence or presence of ISO (Table S1). Next, the inducibility of Ca^{2+} waves was examined in both Ser96 and Ala96 myocytes, in the absence and presence of ISO (1 μmol/L). In the absence of ISO, no cardiomyocytes from either Ser96 or Ala96 mice showed Ca^{2+} waves. However, under ISO (1 μmol/L) and high-frequency (5 Hz) stimulation, Ca^{2+} waves were developed in 50% (10 of 20) of Ala96 cardiomyocytes, compared with 5% (1 of 20) of Ser96 cells (Figure 4C and 4D). Recent studies suggest that RyR-mediated leak occurs in part as Ca^{2+} sparks, although there is RyR-mediated and Ca^{2+} spark–independent leak.[34] Therefore, total SR Ca^{2+} leak was also measured using the tertacaine protocol[4] in the presence of 100 nmol/L ISO (Figure 4E and 4F). The ratio of SR Ca^{2+} leak to SR Ca^{2+} load was larger in Ala96, compared with Ser96 cardiomyocytes (Figure 4G). The increased SR Ca^{2+} leak was

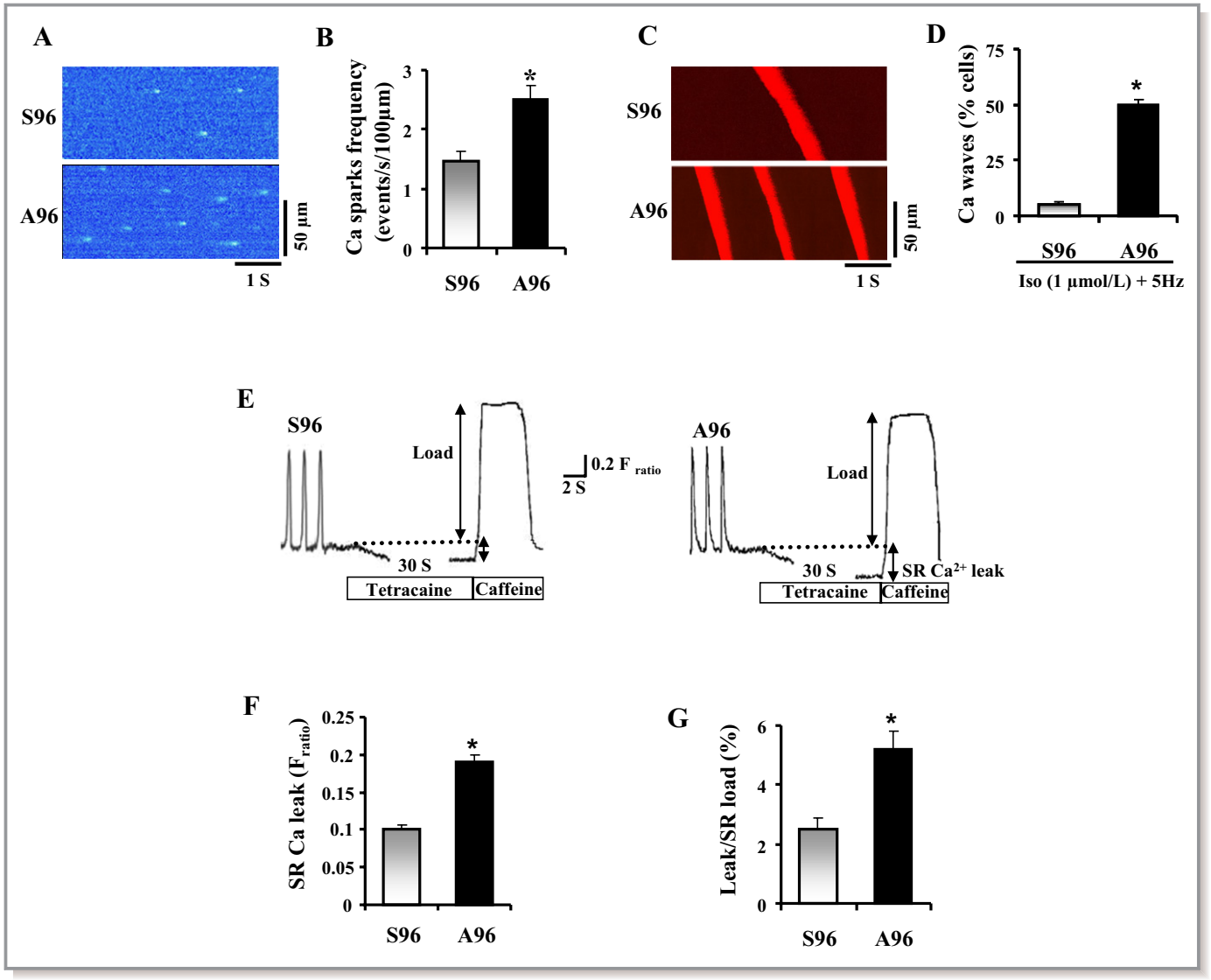

Figure 4. Ca^{2+} sparks and waves in intact Ser96 (S96) and Ala96 (A96) HRC cardiomyocytes. A, Representative line-scan images of Ca^{2+} sparks acquired in Ser96 and Ala96 cardiomyocytes in the presence of 100 nmol/L isoproterenol. B, Cumulative data on Ca^{2+} spark frequency in the presence of 100 nmol/L isoproterenol (n=55 Ser96 cells from 5 hearts and n=61 Ala96 cells from 5 hearts). *P<0.05, Ser96 vs Ala96 (t test). C, Representative line-scan images of Ca^{2+} waves acquired in Ser96 and Ala96 cardiomyocytes in the presence of 1 μmol/L isoproterenol and 5 Hz. D, percentage of cells showing waves (n=20 cells for 3 Ser96 hearts; n=20 cells for 3 Ala96 hearts). *P<0.05, Ser96 vs Ala96 (Fisher Exact test). E, SR Ca^{2+} leak measurements in Ser96 and Ala96 HRC myocytes in the presence of 100 nmol/L isoproterenol. SR Ca^{2+} leak was determined as the tertacaine sensitive drop in diastolic Fura-2 ratio. F, Comparison of average SR Ca^{2+} leak (ratio of twitch Ca^{2+} transient/caffeine-induced Ca^{2+} transient) G, Bar graph showing quantification of leak/SR load relationship in Ser96 and Ala96 HRC myocytes. Ser96 HRC myocytes, n=22 from 3 hearts; Ala96 HRC myocytes, n=28 from 3 hearts. *P<0.05, Ser96 vs Ala96 (Fisher Exact test). HRC indicates histidine-rich Ca^{2+} binding; ISO, isoproterenol; SR, sarcoplasmic reticulum.

associated with enhanced opening of the SR Ca^{2+} release channel in Ala96, as determined by [^{3}H]ryanodine binding in homogenates of Ser96 and Ala96 HRC hearts (Figure S2). Taken together, these findings suggest that expression of Ala96 HRC enhances the propensity for spontaneous Ca^{2+} release from the SR by increasing the activity of the RyR2 channel.

Stress Induced Aftercontractions and DADs in Ala96 Cardiomyocytes

To determine the effects of stress conditions in Ala96 HRC cells, we next measured membrane potentials in cardiomyocytes from Ala96 and Ser96 mice at 5-Hz field stimulation in the presence of 1 μmol/L ISO. Spontaneous aftercontractions occurred in 65% of Ala96 cells within 5 seconds after pacing was stopped, compared with 12% of Ser96 HRC cells (Figure 5A and 5B). Previous studies suggested that aberrant RyR Ca^{2+} release may induce arrhythmias by activation of DADs.[18] To determine whether the mechanism for the arrhythmias elicited by Ala96 HRC is related to DADs, electrical activity was examined under increased frequency of stimulation (5 Hz) in the presence of 1 μmol/L ISO in isolated cardiomyocytes. We compared the action potential duration (APD) of Ser96 and Ala96 cells at 5 Hz and 35°C. No significant differences were detected in the APD90, in the APD50, in the amplitude of AP, and in the resting potential between the 2 groups (Table S2). However, in the presence of 1 μmol/L ISO, 70% of the Ala96 cells developed DADs within 2 to 5 seconds after termination of 5-Hz stimulation, compared with 20% of the Ser96 HRC cells (Figure 5C and 5D). Overall, cellular arrhythmias were significantly more common in Ala96 versus Ser96 cardiomyocytes.

Ala96 Does Not Alter the HRC Ca^{2+}-binding Properties but Decreases Its Interaction With Triadin

To determine the mechanisms associated with impaired Ca^{2+} cycling by Ala96 HRC, we compared its Ca^{2+}-binding properties to those with Ser96 HRC. SR-enriched membrane

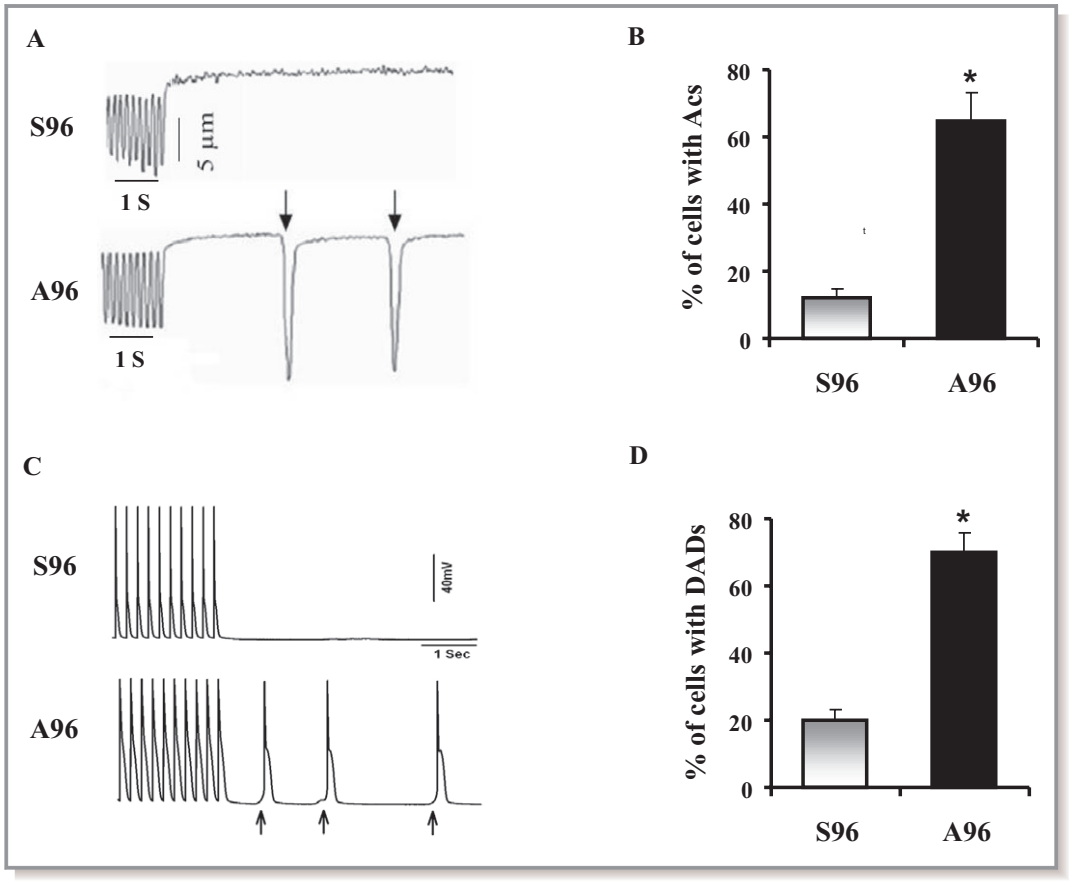

Figure 5. Aftercontractions (Acs) and DADs in Ser96 (S96) and Ala96 (A96) HRC cardiomyocytes at 5-Hz and 1-μmol/L isoproterenol stimulation. A, Representative traces of Acs in Ser96 and Ala96 cardiomyocytes. B, Percentage of the Ser96 and Ala96 cardiomyocytes that developed Acs (n=55 cells for 5 Ser96 hearts; n=68 cells for 5 Ala96 hearts). C, Representative traces of action potential in Ser96 and Ala96 cells. D, Percentage of the Ser96 and Ala96 cells that showed DADs (n=14 cells for 4 Ser96 hearts; n=15 for 5 Ala96 hearts). Acs (A) and DADs (C) are marked with arrows. Data are mean±SEM of the total number of cells/group. *P<0.05 vs Ser96 (Fisher Exact test was used to calculate statistical significance). DADs indicates delayed afterdepolarizations; HRC, histidine-rich Ca^{2+} binding; SEM, standard error of the mean.

fractions of Ser96 and Ala96 HRC were isolated, and their Ca^{2+}-binding affinities were examined using the Ca^{2+} overlay method.[23] At all protein levels tested, the degree of Ca^{2+} binding was similar between Ala96 and Ser96 HRC, indicating that the Ala96 variation in HRC does not alter its Ca^{2+}-binding properties (Figure S3). We then examined whether Ala96 alters the HRC interaction with triadin in the RyR complex.[11,35] Thus, we performed coimmunoprecipitation assays, using antibodies against human HRC in cardiac homogenates of Ser96 and Ala96 HRC mice. The interaction between Ala96 HRC and triadin was weaker compared with Ser96 HRC and triadin (Figure 6A and 6B). We also explored the binding of HRC and triadin under high (0.1 mmol/L) and low (0.1 μmol/L) Ca^{2+}, using purified recombinant proteins. Quantification of immunoblots revealed that the interaction of HRC and triadin was Ca^{2+} dependent for Ser96 HRC but Ca^{2+} independent for Ala96 HRC. Furthermore, Ala96 reduced binding to triadin at both high and low Ca^{2+} (Figure 6C and 6D). Thus, Ala96 does not alter the Ca^{2+}-binding properties of HRC, but it reduces the interaction between HRC and triadin.

Increased Ca^{2+} Spark Frequency and Ca^{2+} Waves in Ala96 Are Associated With Phosphorylation of RyR2

We then examined whether the aberrant Ca^{2+} handling in Ala96 HRC cardiomyocytes was associated with increases in the phosphorylation of RyR2. Previous studies have shown that enhanced phosphorylation of Ser2808 (PKA site) and Ser2814 (CaMKII site) in RyR can modulate RyR2 function.[36,37] Thus, we assessed the phosphorylation state of RyR2 in Ala96 cardiomyocytes, by performing Western blots with phospho-specific antibodies against the RyR2 S2808 and S2814 sites under basal conditions and following ISO stimulation (100 nmol/L) of perfused hearts. Ala96 hearts had significantly increased phosphorylation levels of RyR at

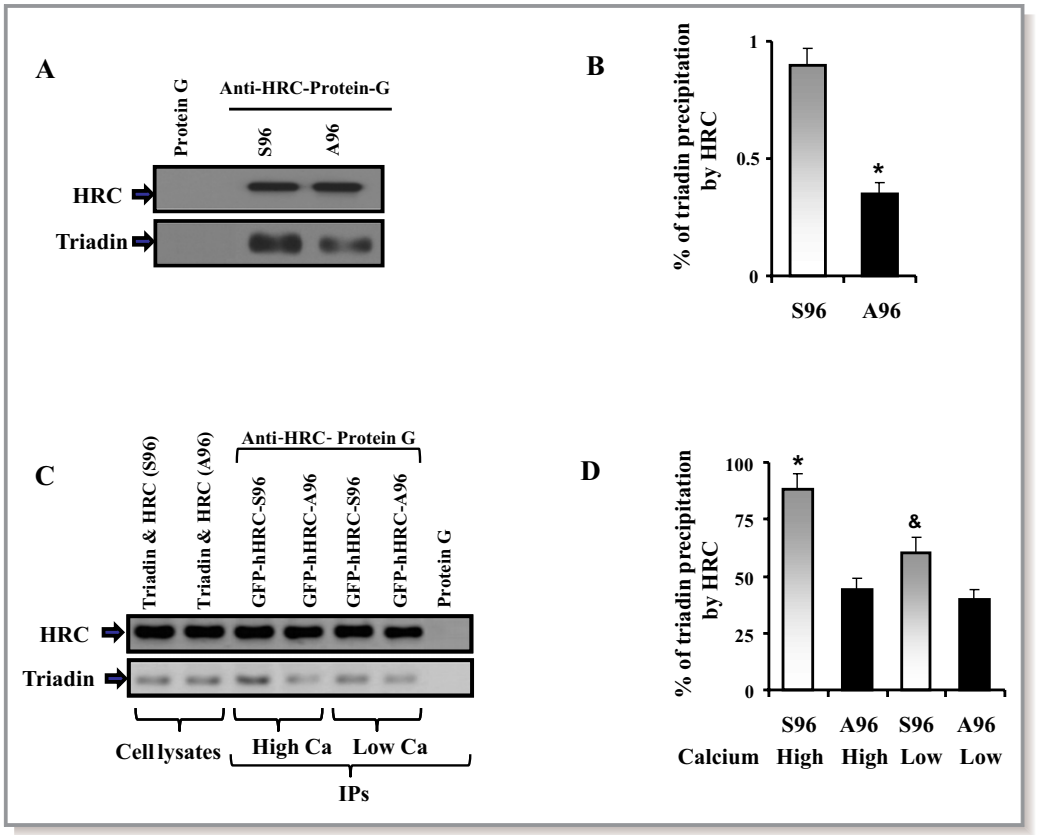

Figure 6. Ala96 (A96) HRC reduces binding to triadin. A, The anti-HRC antibody, coupled to protein G–agarose beads, was used for coimmunoprecipitation of triadin from cardiac homogenates (1 mg total protein) of Ser96 (S96) and Ala96 HRC mice. The precipitates were analyzed by immunoblotting with anti-HRC and anti-TRD antibodies, as indicated. C, Coimmunoprecipitation of triadin from HEK293 cells that coexpressed triadin and Ser96 or Ala96 HRC, under high Ca^{2+} (0.1 mmol/L) and low Ca^{2+} (0.1 μmol/L) conditions was also performed using anti-HRC antibody, coupled to protein G–agarose beads. Top panel: immunoblotting with HRC antibodies; Bottom panel: immunoblotting with triadin antibodies. Immunoprecipitate with anti-IgG PLUS agarose was used as negative control (A and C). B and D, The summary of interactions is presented. Ala96, N=3; Ser96, N=3. *P<0.05, Ala96 vs Ser96 mice (t test); $^{\&}P$<0.05, Ser96 low vs high Ca^{2+} (comparisons were performed by using 1-way ANOVA). ANOVA indicates analysis of variance; GFP, green fluorescent protein; HRC, histidine-rich Ca^{2+} binding; IPs, immunoprecipitations; TRD, Triadin.

S2814, but not at S2808, at baseline and after ISO stimulation (Figure 7A through 7C). The involvement of CaMKII in phosphorylation of S2814 in RyR2 was further confirmed by the ability of KN93, a CaMKII inhibitor, to prevent phosphorylation at this site. Importantly, KN93 blunted the ISO-induced increase in phosphorylation of

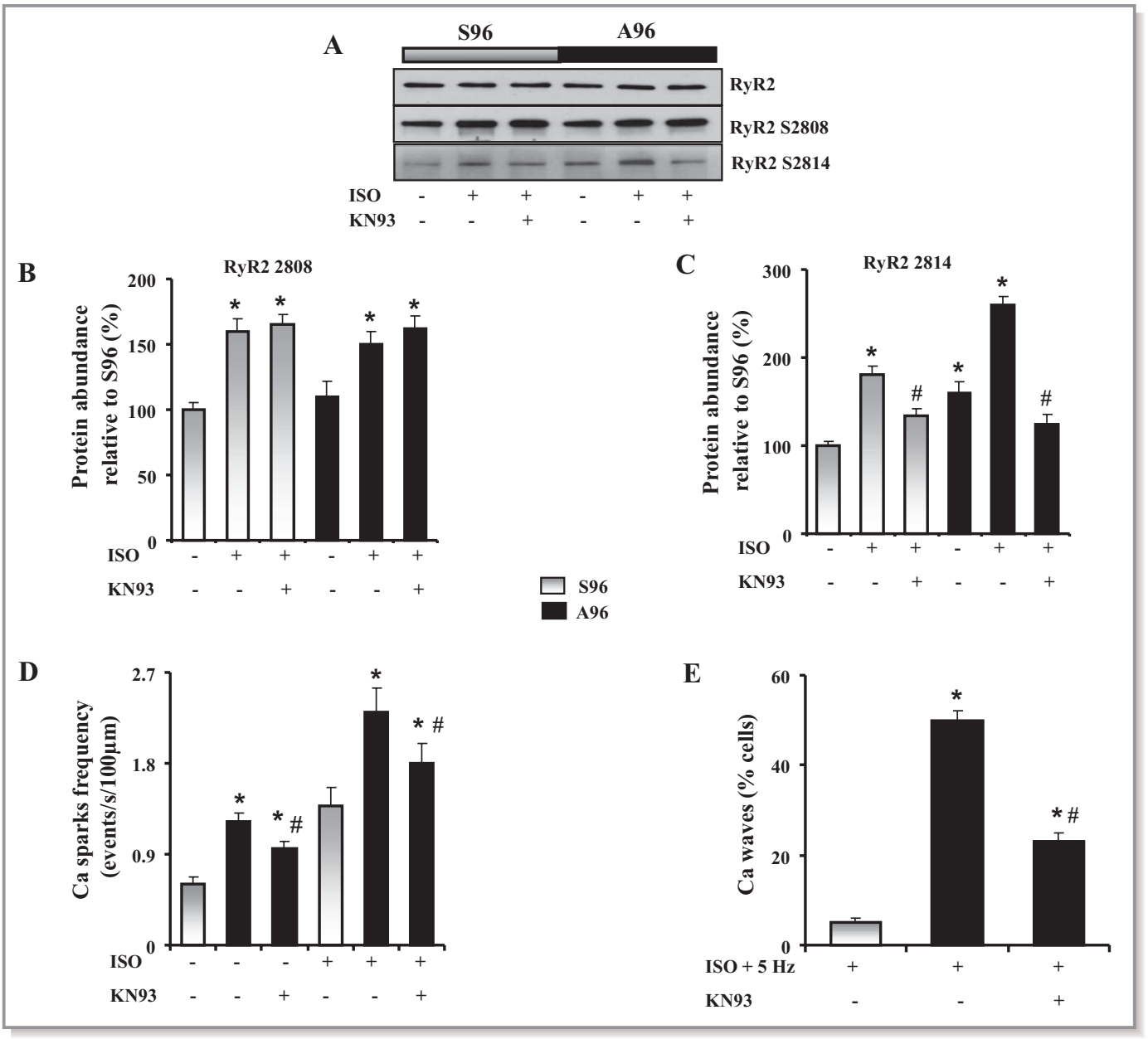

Figure 7. CaMKII-dependent RyR2 phosphorylation and Ca^{2+} sparks/waves in Ser96 (S96) and Ala96 (A96) HRC hearts. A, Representative western blots of protein levels and phosphorylation of RyR2. Total protein homogenates from the left ventricle were used for western blots. Hearts were perfused in the absence or presence of β-adrenergic agonist (100 nmol/L ISO) and/or CaMKII inhibitor (1 μmol/L KN93) with a modified HEPES-Tyrode's solution prior to isolation of the left ventricles. RyR2 phosphorylation at sites S2808 and S2814 was determined with phospho-specific antibodies. B and C, Bar graph showing quantification of ryanodine receptor phosphorylation at S2808 and S2814 sites in the absence (−) or presence of ISO and KN93. Actin was used to verify the amount of loaded samples. Two-way repeated-measures ANOVA were used to compare groups. Values are mean±SEM; N=5 hearts/group. *P<0.05 vs Ser96 (−ISO), #P<0.05 vs Ala96 (±ISO). D, Ca^{2+} spark frequency recorded in Ser96 and Ala96 HRC cardiomyocytes in the absence (basal) or presence of ISO (100 nmol/L) and in the absence or presence of CaMKII inhibitor KN93 (1 μmol/L). E, Percentage of increases in Ca^{2+} waves acquired in Ser96 and Ala96 HRC cardiomyocytes in the presence of 1 μmol/L isoproterenol plus 5 Hz and in the absence or presence of CaMKII inhibitor KN93 (1 μmol/L). For Ca^{2+} sparks: n=32 to 35 cells (−ISO) and n=20 to 28 cells (+ISO); and for Ca^{2+} waves: n=24 to 32 cells. A total of 4 to 5 hearts were used/group. Two-way repeated-measures ANOVA were used to compare groups. *P<0.05 vs Ser96; #P<0.05 vs Ala96. ANOVA indicates analysis of variance; HRC, histidine-rich Ca^{2+} binding; ISO, isoproterenol; RyR2, ryanodine receptor.

S2814 without any effect on phosphorylation of S2808 (Figure 7C). We then examined the contribution of RyR2 phosphorylation by CaMKII in the Ala96-induced increases of Ca^{2+} sparks and waves, using KN93. Inhibition of CaMKII by KN93 significantly prevented the increases in spark frequency under both basal and ISO stimulation conditions (Figure 7D). However, spark frequency remained significantly elevated even in the presence of KN93 (with or without ISO; Figure 7D), indicating that the aberrant SR Ca^{2+} release was partially contributed by the increased CaMKII phosphorylation of RyR. Furthermore, KN93 significantly attenuated the ISO-induced Ca^{2+} waves, elicited by Ala96 HRC (Figure 7E). These findings reveal an additional regulatory mechanism by the Ala96 HRC variant, impacting S2814 phosphorylation of RyR2 and eliciting arrhythmias through this process.

Ala96 HRC Mice Have an Increased Incidence of Ventricular Ectopy on Catecholamine Challenge

We previously reported that the human HRC genetic variant (Ser96Ala) was associated with fatal arrhythmias in DCM patients.[14] Thus, we subjected the Ala96 HRC mice to catecholaminergic stress to determine whether that would induce cardiac arrhythmias in vivo. To test this, the surface ECG was monitored on intraperitoneal injection of ISO. ISO caused frequent premature ventricular complexes in the form of bigeminy and trigeminy (Figure 8A) and episodes of nonsustained ventricular tachycardia in Ala96 mice (Figure 8B). Arrhythmias typically began 3 to 5 minutes after catecholamine injection and lasted 20 minutes into recovery. Of 8 Ala96 mice, 4 displayed nonsustained ventricular tachycardia, while none of the Ser96 HRC mice showed nonsustained ventricular tachycardia events (Figure 8C). Although all VT events were monomorphic, heart rates never exceeded 1000 bpm, and VT rhythms never deteriorated to ventricular fibrillation. The Ser96 mice showed only benign and expected arrhythmias under stress conditions, such as infrequent atrial premature contractions.

Ala96 HRC Mice Exhibit Arrhythmias Associated With Ventricular Tachycardia After MI

To further examine susceptibility to stress conditions, we subjected Ser96 and Ala96 HRC mice to MI in vivo.

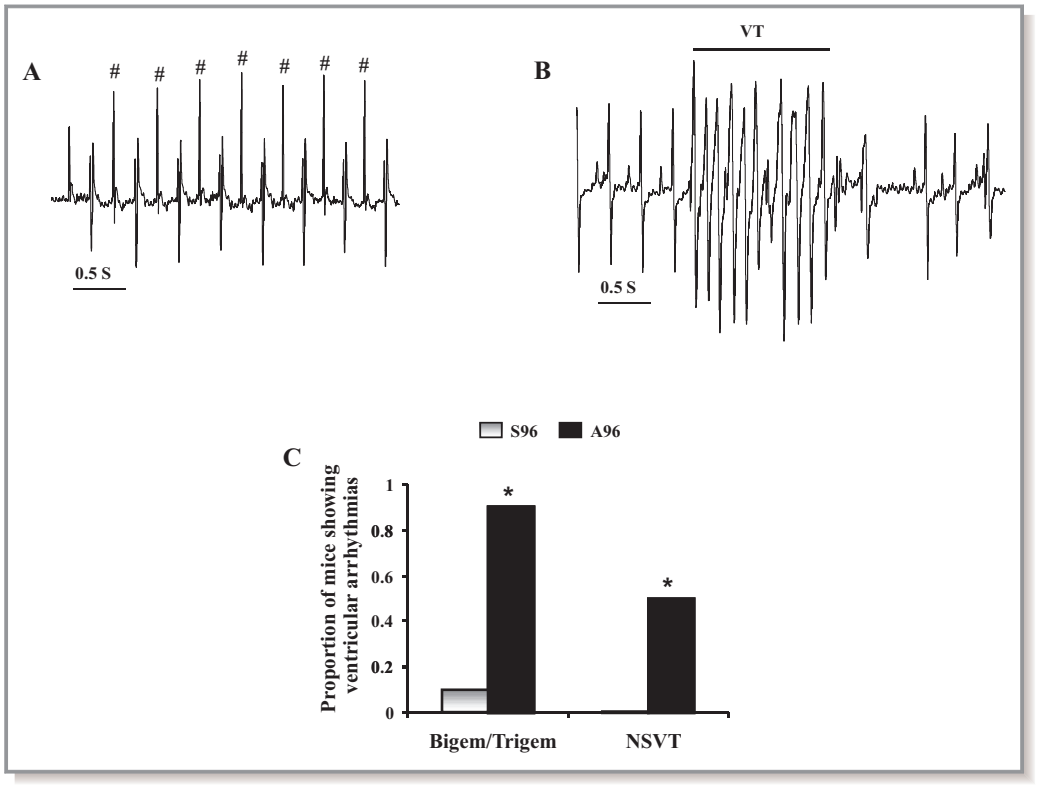

Figure 8. Ala96 (A96) HRC mice display increased ventricular ectopy after catecholamine challenge. A and B, Representative examples of ECG traces showing premature ventricular complexes (PVCs, #) (A) and nonsustained ventricular tachycardia (NSVT, B) in anesthetized Ala96 mice after intraperitoneal injection of isoproterenol (2 mg/kg). C, A high proportion of mice expressing Ala96 displayed complex forms of ventricular arrhythmias (bigeminy/trigeminy and NSVT), compared with Ser96 (S96) mice, following isoproterenol injection. n=8 Ala96 mice; n=8 Ser96 mice. *P<0.05 vs Ser96, the Mann–Whitney U test was used to compare absolute PVC incidence and Fisher exact test was used to evaluate ventricular tachycardia incidence. ECG indicates electrocardiogram; HRC, histidine-rich Ca^{2+} binding.

Interestingly, we observed a marked difference in reperfusion arrhythmias between these groups (Figure 9), as revealed by telemeter ECG transmitters that were implanted 1 week before MI. During the first 24 hours of reperfusion, VT occurred in 7 of 10 Ala96 HRC mice (8 to 15 episodes per mouse; 69 total in the 7 mice), while only 1 of 6 Ser96 HRC

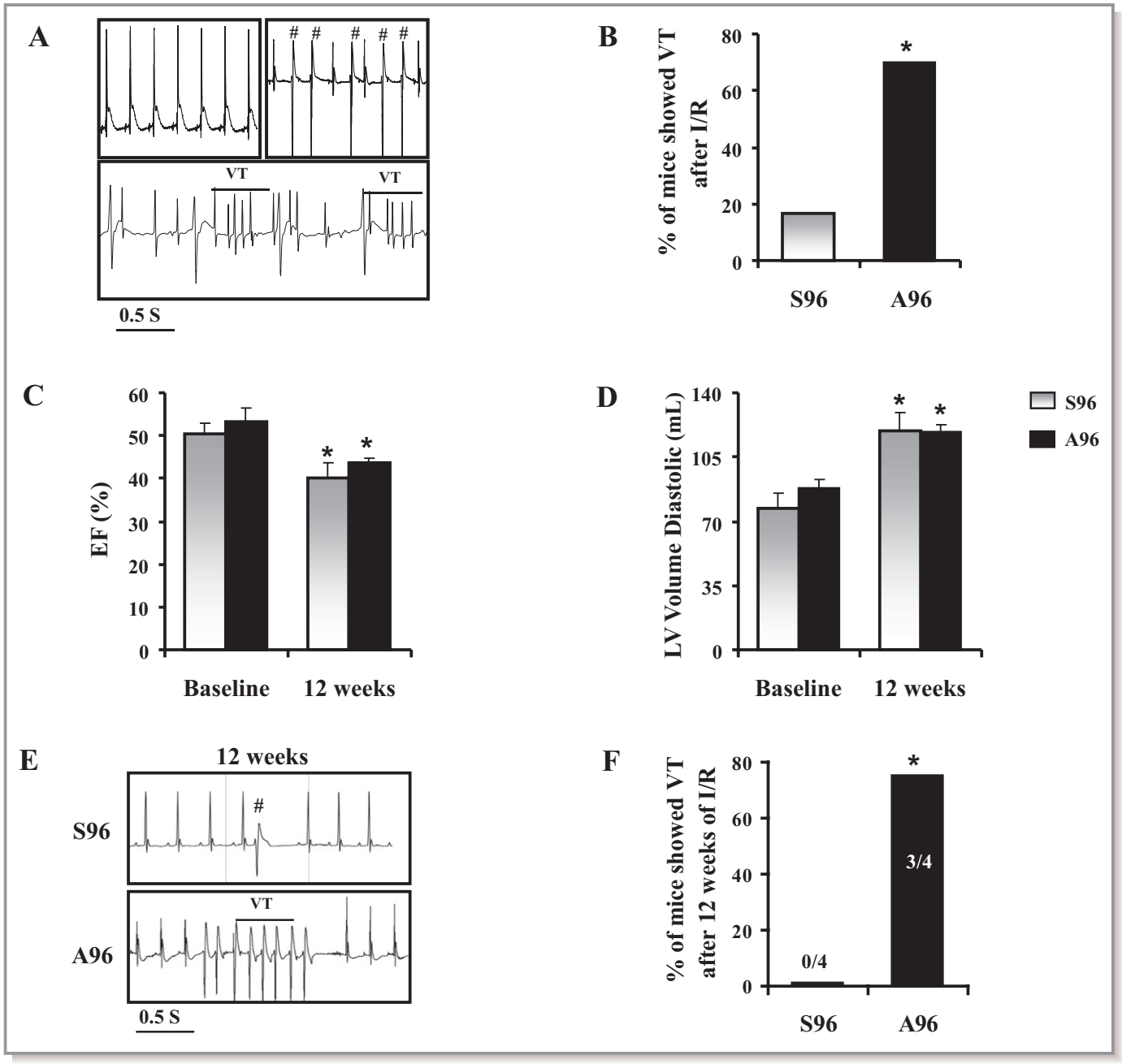

Figure 9. Increased susceptibility to arrhythmias in Ala96 (A96) HRC mice upon myocardial infarction. A, Typical examples of ECG changes during the course of ischemia (top left panel) and representative ECG traces showing ventricular premature beats (#: VPBs, top right panel) and ventricular tachycardia (VT, bottom panel) in an Ala96 HRC mouse after MI. B, Percentage of Ser96 (S96) and Ala96 HRC mice showing VT within 24 hours after MI as monitored by implanted telemeters (N=6 for Ser96 and N=10 for Ala96 mice; *P<0.05 Ala96 vs Ser96). C, Echocardiographic measurements of ejection fraction, and (D) left ventricular diastolic volume in Ser96 (N=4) and Ala96 (N=4) mice at 12 weeks post-MI. *P<0.05 baseline vs 12 weeks (t test). E, Representative telemetry traces depicting (#: VPBs) in a Ser96 mouse and non-sustained ventricular tachycardia (NSVT) in an Ala96 mouse at 12 weeks post MI. F, Bar graph showing incidence of VT in Ser96 and Ala96 mice. VT was observed only in Ala96 mice and in none of the Ser96 mice at 12 weeks after MI. *P<0.05 Ala96 vs Ser96 mice. Fisher exact test was used to evaluate ventricular tachycardia incidence. ECG indicates electrocardiogram; EF, ejection fraction; HRC, histidine-rich Ca^{2+} binding; I/R, ischemia/reperfusion; LV, left ventricle; MI, myocardial infarction.

mice exhibited VT (9 episodes total; $P<0.05$) (Figure 9A and 9B). Furthermore, Kaplan–Meier survival curves showed increased mortality in Ala96 (60%) compared with Ser96 mice (16%; $P<0.05$) during the same time period (data not shown). We then examined whether Ala96 HRC would exacerbate ventricular arrhythmogenesis in DCM, as observed in human carriers.[14] Thus, we extended the post-MI follow-up study in Ala96 and Ser96 HRC mice and monitored function and geometry longitudinally, using echocardiography. At 12 weeks, both groups exhibited significant decreases in ejection fraction and increases in left ventricular cavity dilation (Figure 9C and 9D). These alterations were similar between Ala96 and Ser96 HRC mice. Analysis of telemetry records at 12 weeks post MI indicated that only the Ala96 mice (3 of 4) exhibited spontaneous and prolonged VT, while none (0 of 4) of the Ser96 mice developed VT (Figure 9E and 9F). These data suggest that the presence of "leaky" RyR2 channels, associated with Ala96 HRC, increases the risk for fatal ventricular arrhythmias in DCM carriers.

Discussion

In the current study, we demonstrate for the first time that expression of human Ala96 HRC in vivo results in catecholaminergically mediated malignant arrhythmia associated with enhanced SR Ca^{2+} leak through the ryanodine receptor. The findings indicate that this is the underlying cause of increased risk for sudden cardiac death in DCM patients with Ala96 HRC. Importantly, they suggest that this and other genetic variants in HRC could lie behind cases of idiopathic sudden cardiac death in the general population in the absence of structural cardiac disease.

"Humanized" Ala96 HRC Mouse Exhibits Catecholaminergic Arrhythmia

In end-stage DCM patients, contractile dysfunction is often associated with malignant arrhythmias constituting a major risk factor for sudden cardiac death.[1] These arrhythmias stem mainly from nonreentry mechanisms, such as early afterdepolarizations and DADs, which are linked to impaired cardiomyocyte Ca^{2+} cycling. Interestingly, we observed that human DCM patients with Ser96 HRC were protected from arrhythmias, while Ala96 HRC patients developed fatal arrhythmias.[14] To characterize the underlying mechanisms, we generated humanized HRC mice since there is only 48% homology between human and mouse HRC amino acid sequences.[20] The availability of the HRC-null mouse,[8] allowed us to introduce the human HRC variant proteins (Ser96 or Ala96) in the heart and mimic the human condition. Our findings show that mice bearing the Ala96 HRC present ventricular tachycardia in response to β-adrenergic stimulation in vivo and increased mortality associated with arrhythmias following MI. Quantitative analysis of cardiac dimensions and ultrastructural characterization revealed no structural remodeling, indicating that geometrical alterations were not a contributing factor to arrhythmogenesis in Ala96 HRC mice. Instead, the underlying mechanisms involved (1) enhanced RyR2 leakiness due to decreased binding of HRC to triadin and (2) dysregulated myocyte Ca^{2+} handling manifested in spontaneous Ca^{2+} release and arrhythmogenic DADs.

Mechanism of Ala96 HRC

Our results demonstrating that Ala96 HRC alters Ca^{2+} cycling primarily by compromising normal RyR2 function is based on the following findings. Ala96 HRC increased the fraction of total SR Ca^{2+} released during a twitch and increased the frequency of diastolic Ca^{2+} sparks and Ca^{2+} waves, compared with its Ser96 HRC counterpart. Moreover, we observed enhanced RyR2-mediated SR Ca^{2+} leak in Ala96 HRC myocytes using a tetracaine protocol. The upregulation of both the systolic and diastolic forms of Ca^{2+} release in Ala96 HRC myocytes occurred in the face of a significant decrease in the SR Ca^{2+} content, indicating that stimulated release was not merely a consequence of increased SR Ca^{2+} content. Importantly, the Ala96 HRC cardiomyocytes exhibited aftercontractions and arrhythmogenic DADs, when paced in the presence of β-adrenergic stimulation consistent with the occurrence of cardiac arrhythmias in the Ala96 HRC mice in vivo.

The findings in the Ala96 HRC mouse are also supported by previous studies, which showed that virus-mediated overexpression of HRC depressed SR Ca^{2+} release,[38] whereas knockdown of HRC stimulated Ca^{2+} cycling and increased ryanodine binding in cardiomyocytes.[8,39] Collectively, these results suggest that HRC normally inhibits RyR2 activity and this inhibition is relieved, when HRC is lost or the function of this protein is compromised by genetic mutations. The inhibitory effects of HRC on RyR2 function appear to be mediated though triadin with which HRC interacts.[35] Therefore, the observed upregulation of RyR2 function in Ala96 myocytes could be due to impaired ability of the mutant HRC protein to appropriately interact with triadin. This hypothesis was supported by our protein-binding experiments, which showed that the Ala96 HRC significantly reduced HRC binding to triadin compared with its Ser96 counterpart (Figure 6), leading to RyR2 channels with abnormally high activity, that is, leaky RyR2 (see schematic representation Figure 10).

It is interesting to compare the role of HRC to that of the homologous SR Ca^{2+}-binding protein CASQ2. In addition to serving as an SR Ca^{2+} buffer, CASQ2 regulates RyR2 activity

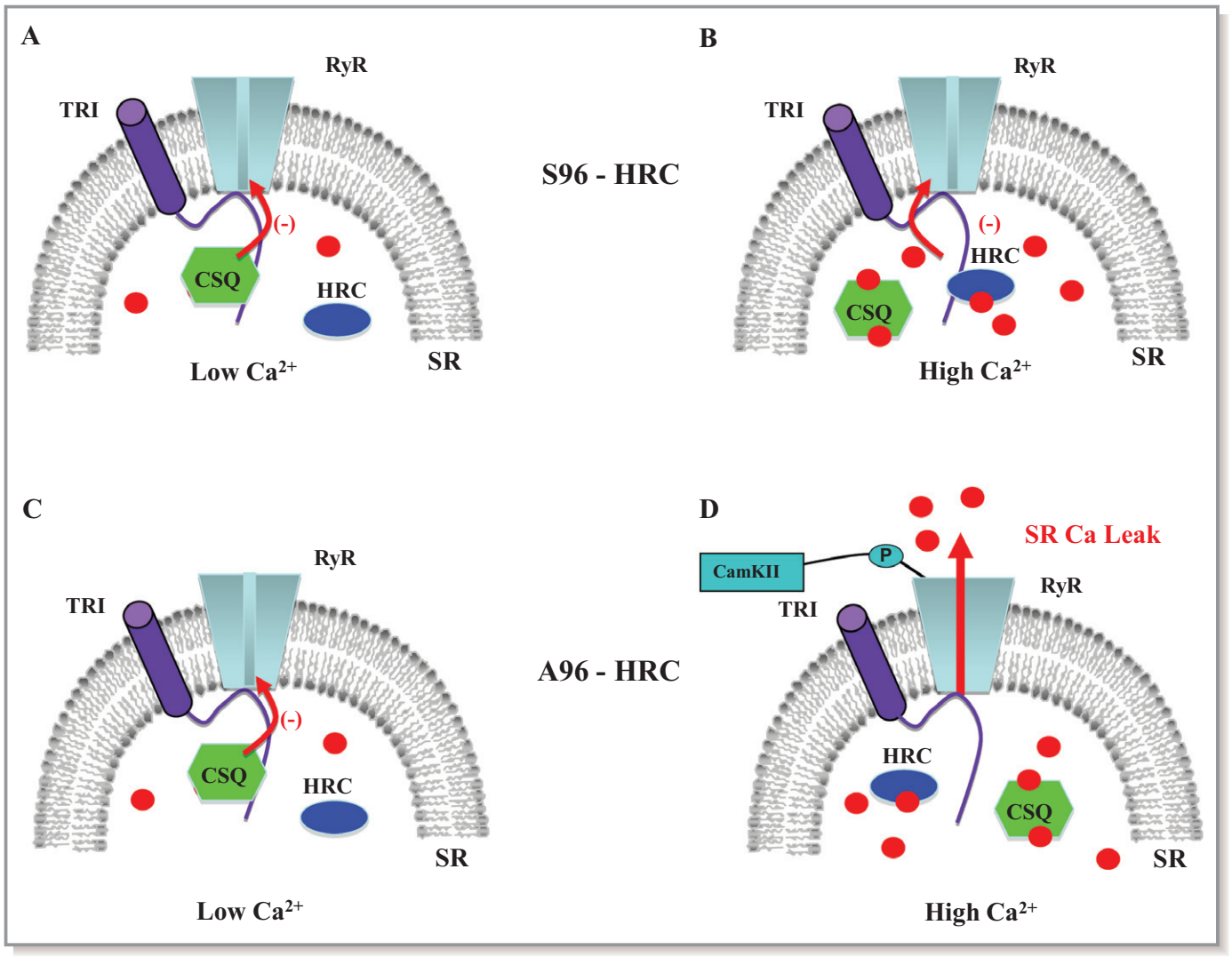

Figure 10. Proposed scheme on the functional interactions between calsequestrin (CSQ), triadin (TRI), histidine-rich Ca^{2+} binding protein (HRC), and ryanodine receptor (RyR) in the cardiac sarcoplasmic reticulum (SR) membrane. In Ser96 (S96) HRC heart, CSQ interacts with TRI, resulting in deactivation of the RyR channel at low luminal Ca^{2+} concentrations, following SR Ca^{2+} release (A). On refilling the SR with Ca^{2+}, CSQ inhibition is relieved as CSQ dissociates from the RyR complex; however, binding of HRC prevents the RyR from becoming leaky (B). In Ala96 (A96) HRC hearts, CSQ interactions are similar to Ser96 HRC at both low and high Ca^{2+} concentrations; however, the interaction of Ala96 HRC with triadin is impaired (C and D), leading to increased RyR2 leak. RyR leakiness is further amplified via phosphorylation by calmodulin-dependent protein kinase II (D).

through interaction with triadin (and junctin).[13,40] Moreover, genetic defects in CASQ2 have been also linked to catecholaminergic polymorphic ventricular tachycardia in human patients.[41] Two of the CSQ mutations were reported to contribute to arrhythmogenesis by impairing interaction of CASQ2 with junctin/triadin in the RyR complex, thereby resulting in impaired regulation of RyR2 by luminal Ca^{2+} and enhanced propensity for spontaneous Ca^{2+} release and DADs.[18,42] Thus, the Ser96Ala variant of HRC may act in a similar manner on RyR2 activity, to increase vulnerability to lethal cardiac arrhythmias.

Notably, at variance with HRC, CASQ2 binds to and inhibits RyR2 at low rather than high luminal Ca^{2+} levels.[40,43] Inhibition of RyR2 at low luminal Ca^{2+} has been shown to contribute to luminal Ca^{2+}-dependent deactivation that helps to keep RyR2 closed after each release but expected to wane as the SR is refilled with Ca^{2+}.[44,45] Our present study suggests that inhibition of RyR2 by HRC provides another level of control over SR Ca^{2+} release expected to operate at high luminal Ca^{2+}, when diastolic Ca^{2+} is restored (and especially when it is elevated above normal levels). Interestingly, HRC has been reported to bind to the same KEKE motive on triadin that CASQ2 binds.[35,46] Thus, Ca^{2+}-dependent regulation of the RyR complex shows an unexpected complexity that could contribute to dynamic regulation of RyR2 function during the Ca^{2+} release–uptake cycle (Figure 10).

Previous studies have shown that phosphorylation of RyR2 by protein kinase A (2808) or CaMKII (Ser2814) increases SR Ca^{2+} leak, although most studies have linked only the CaMKII-dependent phosphorylation of RyR2 with diastolic SR Ca^{2+} leak in heart failure (HF).[37,47] In our study, the alterations of RyR2 function and SR Ca^{2+} release in Ala96 HRC myocytes were associated with increased phosphorylation of RyR2 at the CaMKII site S2814 and not at the PKA site S2808. Furthermore, inhibiting CaMKII with K93 partially reduced the increased RyR2 Ca^{2+} spark rate, both at baseline and after β-adrenergic stimulation (Figure 7). These findings on altered interaction of Ala96 HRC with the RyR2 complex coupled with amplified CaMKII phosphorylation of RyR2 and increased Ca^{2+} leak may constitute the underlying mechanisms for increased propensity of ventricular arrhythmias in vivo under I/R injury or cardiomyopathy conditions in Ala96 HRC mice (Figure 9). Importantly, the current observations in transgenics correlate with previous clinical results, which linked the Ala96 HRC variant to life-threatening ventricular arrhythmias and sudden death in DCM carriers.[14]

In conclusion, a single nucleotide substitution of Thr286Gly in HRC results in a naturally occurring variant (Ala96) that leads not only to depressed SR Ca^{2+} cycling and contractility but also to increased SR Ca^{2+} leak during diastole. The induced diastolic leak by hyperactive RyR2 triggers aftercontractions and DADs in cardiomyocytes under stress conditions, which predisposes to increased ventricular tachycardia in the setting of DCM even in the absence of any structural heart disease. These findings establish a pathological link between the Ala96 variant in HRC gene and the clinical phenotype in DCM carriers. Thus, Ala96 HRC appears to be a context-sensitive human variant, which becomes arrhythmogenic in heart failure conditions. The underlying molecular mechanisms of this variant and the susceptibility to malignant arrhythmias may provide new insights to pathways of excitation–contraction coupling, leading to the development of novel clinical interventions.

Acknowledgments

We wish to thank Jiang Min for echocardiography and Michael Tabet for ryanodine binding protocol assistance.

Sources of Funding

This work was supported by National Institutes of Health grants HL64018 and HL26057 (to Dr Kranias), American Heart Association (postdoctoral fellowship to Dr Singh), GIST Systems Biology Infrastructure Establishment Grant, and the European Community's Seventh Framework Programme FP72007-2013 under grant agreement HEALTH-F2-2009–241526, EUTrigTreat.

Disclosures

None.

References

1. Grimm W, Maisch B. Sudden cardiac death in dilated cardiomyopathy—therapeutic options. *Herz*. 2002;27:750–759.
2. Gregori D, Rosato R, Zecchin M, Baldi I, Di Lenarda A. Heart failure and sudden death in dilated cardiomyopathy: hidden competition we should not forget about when modelling mortality. *J Eval Clin Pract*. 2008;14:53–58.
3. Pogwizd SM, Schlotthauer K, Li L, Yuan W, Bers DM. Arrhythmogenesis and contractile dysfunction in heart failure: roles of sodium-calcium exchange, inward rectifier potassium current, and residual beta-adrenergic responsiveness. *Circ Res*. 2001;88:1159–1167.
4. Shannon TR, Pogwizd SM, Bers DM. Elevated sarcoplasmic reticulum Ca^{2+} leak in intact ventricular myocytes from rabbits in heart failure. *Circ Res*. 2003;93:592–594.
5. Hasenfuss G. Alterations of calcium-regulatory proteins in heart failure. *Cardiovasc Res*. 1998;37:279–289.
6. Györke S, Carnes C. Dysregulated sarcoplasmic reticulum calcium release: potential pharmacological target in cardiac disease. *Pharmacol Ther*. 2008;119:340–354.
7. Suk JY, Kim YS, Park WJ. HRC resides in the lumen of sarcoplasmic reticulum as a multimer. *Biochem Biophys Res Commun*. 1999;263:667–671.
8. Park CS, Chen S, Lee H, Cha H, Oh JG, Hong S, Han P, Ginsburg KS, Jin S, Park I, Singh VP, Wang HS, Franzini-Armstrong C, Park WJ, Bers DM, Kranias EG, Cho C, Kim DH. Targeted ablation of the histidine-rich Ca^{2+}-binding protein (HRC) gene is associated with abnormal SR Ca^{2+}-cycling and severe pathology under pressure-overload stress. *Basic Res Cardiol*. 2013;108:344.
9. Gregory KN, Ginsburg KS, Bodi I, Hahn H, Marreez YM, Song Q, Padmanabhan PA, Mitton BA, Waggoner JR, Del Monte F, Park WJ, Ii GW, Bers DM, Kranias EG. Histidine-rich Ca^{2+} binding protein: a regulator of sarcoplasmic reticulum calcium sequestration and cardiac function. *J Mol Cell Cardiol*. 2006;40:653–665.
10. Arvanitis DA, Vafiadaki E, Fan GC, Mitton BA, Gregory KN, Del Monte F, Kontrogianni-Konstantopoulos A, Sanoudou D, Kranias EG. Histidine-rich Ca^{2+}-binding protein interacts with sarcoplasmic reticulum Ca-ATPase. *Am J Physiol Heart Circ Physiol*. 2007;293:H1581–H1589.
11. Damiani E, Picello E, Saggin L, Margreth A. Identification of triadin and of histidine-rich Ca^{2+}-binding protein as substrates of 60 kDa calmodulin-dependent protein kinase in junctional terminal cisternae of sarcoplasmic reticulum of rabbit fast muscle. *Biochem Biophys Res Commun*. 1995;209:457–465.
12. Sacchetto R, Damiani E, Turcato F, Nori A, Margreth A. Ca^{2+}-dependent interaction of triadin with histidine-rich Ca^{2+}-binding protein carboxyl-terminal region. *Biochem Biophys Res Commun*. 2001;289:1125–1134.
13. Zhang L, Kelley J, Schmeisser G, Kobayashi YM, Jones LR. Complex formation between junctin, triadin, calsequestrin, and the ryanodine receptor. Proteins of the cardiac junctional sarcoplasmic reticulum membrane. *J Biol Chem*. 1997;272:23389–23397.
14. Arvanitis DA, Sanoudou D, Kolokathis F, Vafiadaki E, Papalouka V, Kontrogianni-Konstantopoulos A, Theodorakis GN, Paraskevaidis IA, Adamopoulos S, Dorn GW II, Kremastinos DT, Kranias EG. The Ser96Ala variant in histidine-rich calcium-binding protein is associated with life-threatening ventricular arrhythmias in idiopathic dilated cardiomyopathy. *Eur Heart J*. 2008;29:2514–2525.
15. Han P, Cai W, Wang Y, Lam CK, Arvanitis DA, Singh VP, Chen S, Zhang H, Zhang R, Cheng H, Kranias EG. Catecholaminergic-induced arrhythmias in failing cardiomyocytes associated with human HRCS96A variant overexpression. *Am J Physiol Heart Circ Physiol*. 2011;301:H1588–H1595.
16. Rizzi N, Liu N, Napolitano C, Nori A, Turcato F, Colombi B, Bicciato S, Arcelli D, Spedito A, Scelsi M, Villani L, Esposito G, Boncompagni S, Protasi F, Volpe P, Priori SG. Unexpected structural and functional consequences of the R33Q homozygous mutation in cardiac calsequestrin: a complex arrhythmogenic cascade in a knock in mouse model. *Circ Res*. 2008;103:298–306.
17. Kashimura T, Briston SJ, Trafford AW, Napolitano C, Priori SG, Eisner DA, Venetucci LA. In the RyR2 (R4496C) mouse model of CPVT, β-adrenergic stimulation induces Ca waves by increasing SR Ca content and not by decreasing the threshold for Ca waves. *Circ Res*. 2010;107:1483–1489.
18. Viatchenko-Karpinski S, Terentyev D, Györke I, Terentyeva R, Volpe P, Priori SG, Napolitano C, Nori A, Williams SC, Györke S. Abnormal calcium signaling

and sudden cardiac death associated with mutation of calsequestrin. *Circ Res*. 2004;94:471–477.

19. Roux-Buisson N, Cacheux M, Fourest-Lieuvin A, Fauconnier J, Brocard J, Denjoy I, Durand P, Guicheney P, Kyndt F, Leenhardt A, Le Marec H, Lucet V, Mabo P, Probst V, Monnier N, Ray PF, Santoni E, Trémeaux P, Lacampagne A, Fauré J, Lunardi J, Marty I. Absence of triadin, a protein of the calcium release complex, is responsible for cardiac arrhythmia with sudden death in human. *Hum Mol Genet*. 2012;21:2759–2767.
20. Hofmann SL, Topham M, Hsieh CL, Francke U. cDNA and genomic cloning of HRC, a human sarcoplasmic reticulum protein, and localization of the gene to human chromosome 19 and mouse chromosome 7. *Genomics*. 1991;9: 656–669.
21. Zhao W, Yuan Q, Qian J, Waggoner JR, Pathak A, Chu G, Mitton B, Sun X, Jin J, Braz JC, Hahn HS, Marreez Y, Syed F, Pollesello P, Annila A, Wang HS, Schultz Jel J, Molkentin JD, Liggett SB, Dorn GW II, Kranias EG. The presence of Lys27 instead of Asn27 in human phospholamban promotes sarcoplasmic reticulum Ca^{2+}-ATPase superinhibition and cardiac remodeling. *Circulation*. 2006;113: 995–1004.
22. Li L, Chu G, Kranias EG, Bers DM. Cardiac myocyte calcium transport in phospholamban knockout mouse: relaxation and endogenous CaMKII effects. *Am J Physiol*. 1998;274:H1335–H1347.
23. Zorzato F, Volpe P. Calcium binding proteins of junctional sarcoplasmic reticulum: detection by 45Ca ligand overlay. *Arch Biochem Biophys*. 1988;261: 324–329.
24. Kirchhefer U, Wehrmeister D, Postma AV, Pohlentz G, Mormann M, Kucerova D, Müller FU, Schmitz W, Schulze-Bahr E, Wilde AA, Neumann J. The human CASQ2 mutation K206N is associated with hyperglycosylation and altered cellular calcium handling. *J Mol Cell Cardiol*. 2010;49:95–105.
25. Campbell KP, MacLennan DH, Jorgensen AO. Staining of the Ca^{2+}-binding proteins, calsequestrin, calmodulin, troponin C, and S-100, with the cationic carbocyanine dye "Stains-all". *J Biol Chem*. 1983;25:11267–11273.
26. Yuan Q, Fan G, Dong M, Altschafl B, Diwan A, Ren X, Hahn H, Zhao W, Waggoner J, Jones L, Jones W, Bers D, Dorn GW II, Wang H, Valdivia H, Chu G, Kranias EG. Sarcoplasmic reticulum calcium overloading in junctin deficiency enhances cardiac contractility but increases ventricular automaticity. *Circulation*. 2007;115:300–309.
27. Yan S, Chen Y, Dong M, Song W, Belcher SM, Wang HS. Bisphenol A and 17β-estradiol promote arrhythmia in the female heart via alteration of calcium handling. *PLoS One*. 2011;6:e25455.
28. Fan GC, Ren X, Qian J, Yuan Q, Nicolaou P, Wang Y, Jones WK, Chu G, Kranias EG. Novel cardioprotective role of a small heat-shock protein, Hsp20, against ischemia/reperfusion injury. *Circulation*. 2005;111:1792–1799.
29. Qian J, Ren X, Wang X, Zhang P, Jones WK, Molkentin JD, Fan GC, Kranias EG. Blockade of Hsp20 phosphorylation exacerbates cardiac ischemia/reperfusion injury by suppressed autophagy and increased cell death. *Circ Res*. 2009;105:1223–1231.
30. Chopra N, Kannankeril PJ, Yang T, Hlaing T, Holinstat I, Ettensohn K, Pfeifer K, Akin B, Jones LR, Franzini-Armstrong C, Knollmann BC. Modest reductions of cardiac calsequestrin increase sarcoplasmic reticulum Ca^{2+} leak independent of luminal Ca^{2+} and trigger ventricular arrhythmias in mice. *Circ Res*. 2007;101:617–626.
31. el-Hayek R, Lokuta AJ, Arévalo C, Valdivia HH. Peptide probe of ryanodine receptor function. Imperatoxin A, a peptide from the venom of the scorpion Pandinus imperator, selectively activates skeletal-type ryanodine receptor isoforms. *J Biol Chem*. 1995;48:28696–28704.
32. Fan G, Chu G, Mitton B, Song Q, Yuan Q, Kranias E. Small heat-shock protein Hsp20 phosphorylation inhibits beta-agonist-induced cardiac apoptosis. *Circ Res*. 2004;94:1474–1482.
33. Wehrens XH, Lehnart SE, Reiken S, van der Nagel R, Morales R, Sun J, Cheng Z, Deng SX, de Windt LJ, Landry DW, Marks AR. Enhancing calstabin binding to ryanodine receptors improves cardiac and skeletal muscle function in heart failure. *Proc Natl Acad Sci USA*. 2005;102:9607–9612.
34. Zima AV, Bovo E, Bers DM, Blatter LA. Ca^{2+} spark-dependent and -independent sarcoplasmic reticulum Ca^{2+} leak in normal and failing rabbit ventricular myocytes. *J Physiol*. 2010;588:4743–4757.
35. Lee HG, Kang H, Kim DH, Park WJ. Interaction of HRC and triadin in the lumen of sarcoplasmic reticulum. *J Biol Chem*. 2001;276:39533–39538.
36. Shan J, Betzenhauser MJ, Kushnir A, Reiken S, Meli AC, Wronska A, Dura M, Chen BX, Marks AR. Role of chronic ryanodine receptor phosphorylation in heart failure and β-adrenergic receptor blockade in mice. *J Clin Invest*. 2010;120:4375–4387.
37. van Oort RJ, McCauley MD, Dixit SS, Pereira L, Yang Y, Respress JL, Wang Q, De Almeida AC, Skapura DG, Anderson ME, Bers DM, Wehrens XH. Ryanodine receptor phosphorylation by calcium/calmodulin-dependent protein kinase II promotes life-threatening ventricular arrhythmias in mice with heart failure. *Circulation*. 2010;122:2669–2679.
38. Fan GC, Gregory KN, Zhao W, Park WJ, Kranias EG. Regulation of myocardial function by histidine-rich, calcium-binding protein. *Am J Physiol Heart Circ Physiol*. 2004;287:H1705–H1711.
39. Park CS, Cha H, Kwon EJ, Jeong D, Hajjar RJ, Kranias EG, Cho C, Park WJ, Kim DH. AAV-mediated knock-down of HRC exacerbates transverse aorta constriction-induced heart failure. *PLoS One*. 2012;7:e43282.
40. Györke I, Hester N, Jones LR, Györke S. The role of calsequestrin, triadin, and junctin in conferring cardiac ryanodine receptor responsiveness to luminal calcium. *Biophys J*. 2004;86:2121–2128.
41. Laitinen PJ, Swan H, Kontula K. Molecular genetics of exercise-induced polymorphic ventricular tachycardia: identification of three novel cardiac ryanodine receptor mutations and two common calsequestrin 2 amino-acid polymorphisms. *Eur J Hum Genet*. 2003;11:888–891.
42. Terentyev D, Nori A, Santoro M, Viatchenko-Karpinski S, Kubalova Z, Gyorke I, Terentyeva R, Vedamoorthyrao S, Blom NA, Valle G, Napolitano C, Williams SC, Volpe P, Priori SG, Gyorke S. Abnormal interactions of calsequestrin with the ryanodine receptor calcium release channel complex linked to exercise-induced sudden cardiac death. *Circ Res*. 2006;98:1151–1158.
43. Beard NA, Casarotto MG, Wei L, Varsányi M, Laver DR, Dulhunty AF. Regulation of ryanodine receptors by calsequestrin: effect of high luminal $Ca^{2+}$and phosphorylation. *Biophys J*. 2005;88:3444–3454.
44. Stevens SC, Terentyev D, Kalyanasundaram A, Periasamy M, Györke S. Intra-sarcoplasmic reticulum Ca^{2+} oscillations are driven by dynamic regulation of ryanodine receptor function by luminal Ca^{2+} in cardiomyocytes. *J Physiol*. 2009;587:4863–4872.
45. Radwański PB, Belevych AE, Brunello L, Carnes CA, Györke S. Store-dependent deactivation: cooling the chain-reaction of myocardial calcium signaling. *J Mol Cell Cardiol*. 2012;S0022–2828:00376–00378.
46. Arvanitis DA, Vafiadaki E, Sanoudou D, Kranias EG. Histidine-rich calcium binding protein: the new regulator of sarcoplasmic reticulum calcium cycling. *J Mol Cell Cardiol*. 2011;50:43–49.
47. Guo T, Zhang T, Mestril R, Bers DM. CaMKII phosphorylation of ryanodine receptor does affect calcium sparks in mouse ventricular myocytes. *Circ Res*. 2006;99:398–406.

	Spark Frequency (events/s/100µm)	Amplitude (F/F0)	FWHM (µm)	FDHM (ms)	N (Sparks/cells/ mice)
S96	0.7	1.69	1.88	30	195/35/6
A96	1.20*	1.72	1.91	31	240/34/6
S96 + Iso	1.45$^{\alpha}$	2.0	2.20	35	455/55/5
A96 + ISo	2.5* $^{\alpha}$	2.3	2.24	36	774/61/5

Supplement Table I: Ca^{2+}-spark characteristics in intact cardiomyocytes in the absence or presence of Iso (100 nmol/L). FWHM: Full width at half maximum; FDHM: Full duration at half maximum. Data are expressed as mean ± SE, *$p<0.05$, S96 vs.A96; α denotes data that are also presented in Figure 3B.

	S96 Myocytes (N=4)	**A96 Myocytes (N=5)**
APD_{90}, ms	97.4±11	104.26 ±10.6
APD_{50}, ms	8.4 ±2.5	8.79 ±2.8
Resting potential, mV	-65.31 ±1.1	-68.38 ±1.2
Amplitude of APD, mV	104.52 ±1.9	112 ±2.2

Supplement Table II: Characteristics of action potential in S96 and A96-HRC cardiomyocytes at 5 Hz and in the presence of 1 μmol/L isoproterenol at 35°C. APD: Action potential duration. Data are expressed as mean ± SE .N represents number of mice (n=14 S96 cells and n=15 A96 cells).

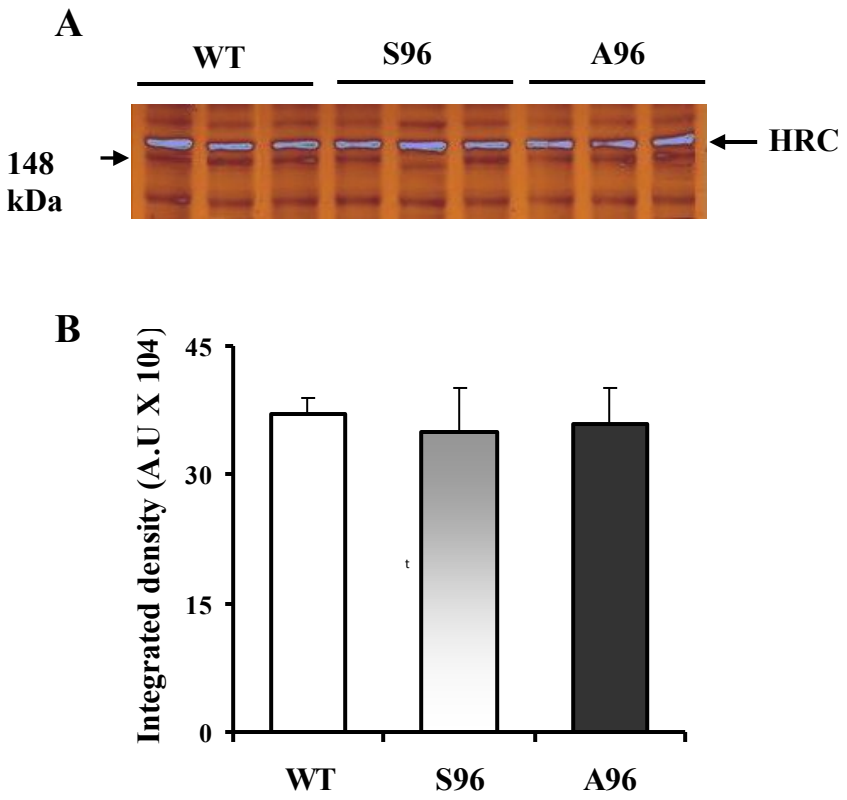

Supplemental figure I

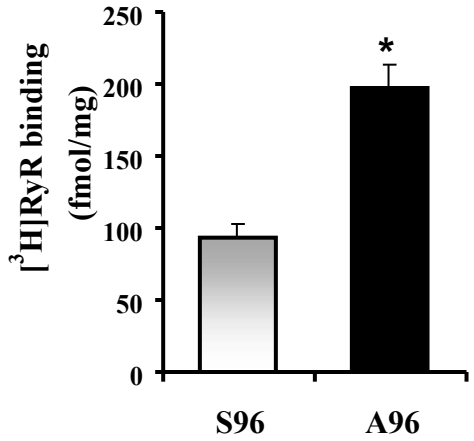

Supplemental figure II

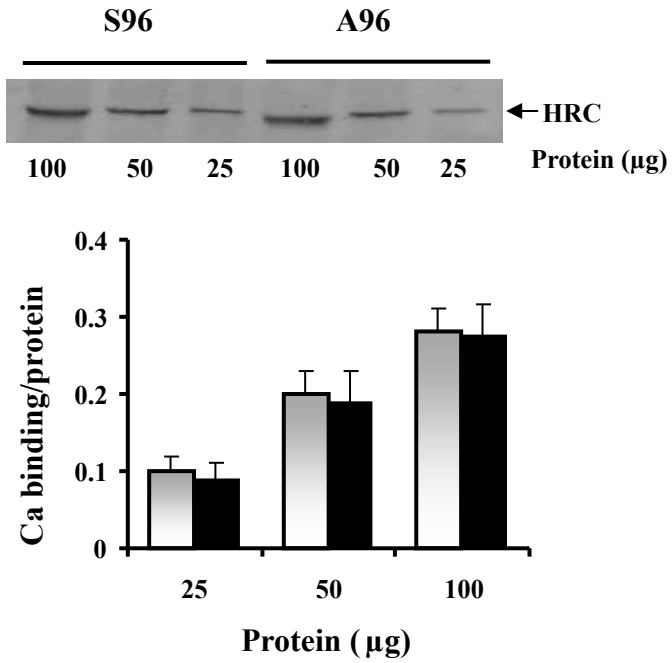

Supplemental figure III

Supplement figure I. Comparison of HRC levels in WT (non-transgenic), S96 and A96-HRC hearts. A, Representative gel of separated proteins by SDS-PAGE and stained with Stains-all (see material and methods in online-only Data Supplement). The blue band at ~160 kDa is HRC. B, Quantification of HRC levels in WT (non-transgenic), S96 and A96 hearts.. Values are mean ± SEM; n= 3 hearts/group.

Supplement figure II. A96-HRC increases RyR binding. [3H] ryanodine binding to Ca^{2+} release channels was determined at saturating conditions in homogenates of S96 and A96-HRC hearts. A96, n=4; S96, n=4. *P<0.05 A96 vs. S96 mice.

Supplement figure III. Enriched SR fractions were isolated from S96 and A96 hearts and different amounts of protein were analyzed by SDS-PAGE. The proteins were transferred to nitrocellulose membranes, which were incubated with $45Ca^{2+}$ in the presence of 1mM $CaCl_2$. A representative autoradiogram (upper panel) and quantified signals (lower panel) are shown. A96, n=3 hearts; S96, n=3 hearts.

Abnormal Calcium Cycling and Cardiac Arrhythmias Associated With the Human Ser96Ala Genetic Variant of Histidine-Rich Calcium-Binding Protein

Vivek P. Singh, Jack Rubinstein, Demetrios A. Arvanitis, Xiaoping Ren, Xiaoqian Gao, Kobra Haghighi, Mark Gilbert, Venkat R. Iyer, Do Han Kim, Chunghee Cho, Keith Jones, John N. Lorenz, Clara F. Armstrong, Hong-Sheng Wang, Sandor Gyorke and Evangelia G. Kranias

J Am Heart Assoc. 2013;2:e000460; originally published October 14, 2013;
doi: 10.1161/JAHA.113.000460
The *Journal of the American Heart Association* is published by the American Heart Association, 7272 Greenville Avenue, Dallas, TX 75231
Online ISSN: 2047-9980

	Spark Frequency (events/s/100µm)	Amplitude (F/F0)	FWHM (µm)	FDHM (ms)	N (Sparks/cells/ mice)
S96	0.7	1.69	1.88	30	195/35/6
A96	1.20*	1.72	1.91	31	240/34/6
S96 + Iso	1.45$^{\alpha}$	2.0	2.20	35	455/55/5
A96 + ISo	2.5* $^{\alpha}$	2.3	2.24	36	774/61/5

Supplement Table I: Ca^{2+}-spark characteristics in intact cardiomyocytes in the absence or presence of Iso (100 nmol/L). FWHM: Full width at half maximum; FDHM: Full duration at half maximum. Data are expressed as mean ± SE, *$p<0.05$, S96 vs.A96; α denotes data that are also presented in Figure 3B.

	S96 Myocytes (N=4)	**A96 Myocytes (N=5)**
APD_{90}, ms	97.4±11	104.26 ±10.6
APD_{50}, ms	8.4 ±2.5	8.79 ±2.8
Resting potential, mV	-65.31 ±1.1	-68.38 ±1.2
Amplitude of APD, mV	104.52 ±1.9	112 ±2.2

Supplement Table II: Characteristics of action potential in S96 and A96-HRC cardiomyocytes at 5 Hz and in the presence of 1 μmol/L isoproterenol at 35°C. APD: Action potential duration. Data are expressed as mean ± SE .N represents number of mice (n=14 S96 cells and n=15 A96 cells).

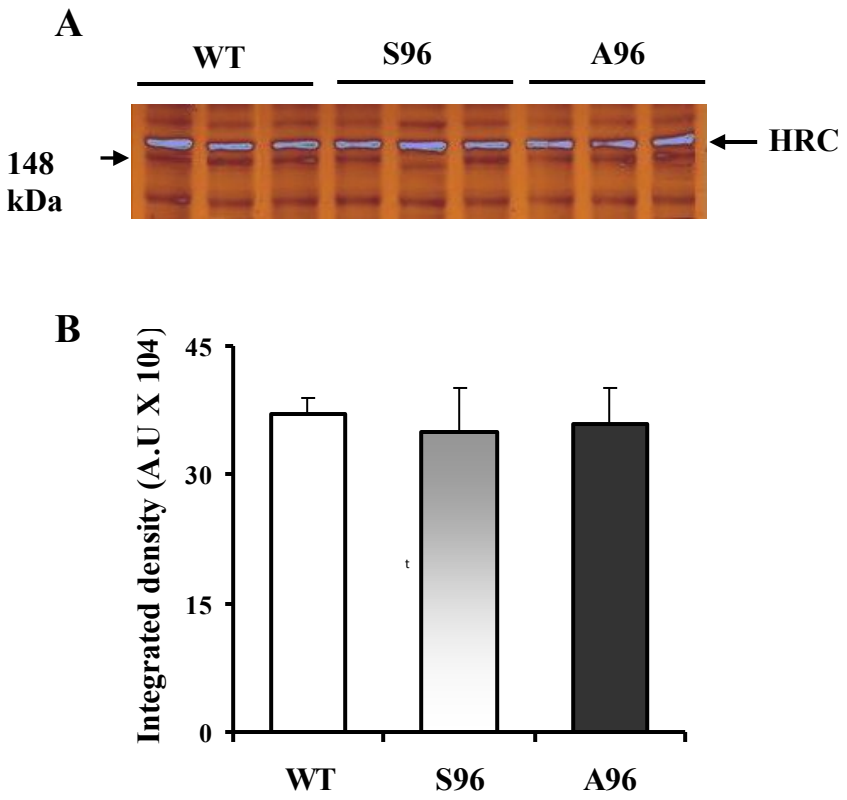

Supplemental figure I

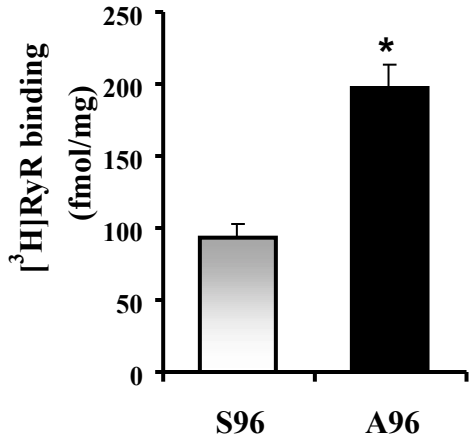

Supplemental figure II

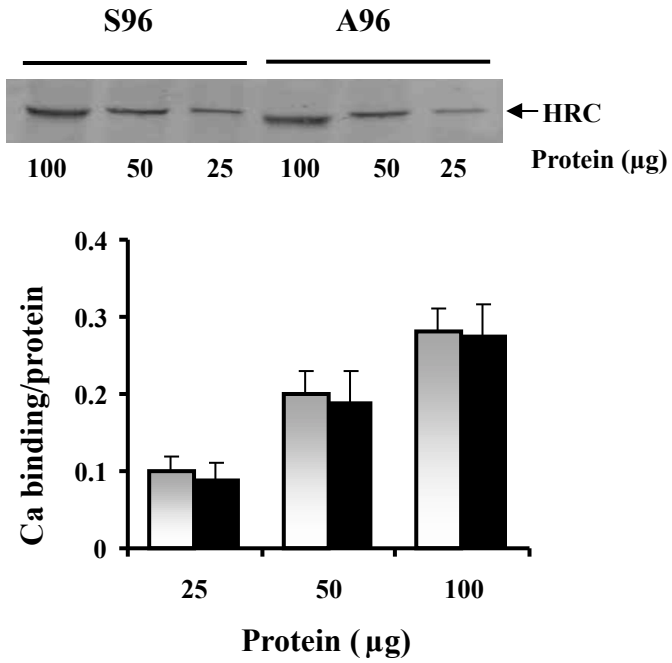

Supplemental figure III

Supplement figure I. Comparison of HRC levels in WT (non-transgenic), S96 and A96-HRC hearts. A, Representative gel of separated proteins by SDS-PAGE and stained with Stains-all (see material and methods in online-only Data Supplement). The blue band at ~160 kDa is HRC. B, Quantification of HRC levels in WT (non-transgenic), S96 and A96 hearts.. Values are mean ± SEM; n= 3 hearts/group.

Supplement figure II. A96-HRC increases RyR binding. [3H] ryanodine binding to Ca^{2+} release channels was determined at saturating conditions in homogenates of S96 and A96-HRC hearts. A96, n=4; S96, n=4. *P<0.05 A96 vs. S96 mice.

Supplement figure III. Enriched SR fractions were isolated from S96 and A96 hearts and different amounts of protein were analyzed by SDS-PAGE. The proteins were transferred to nitrocellulose membranes, which were incubated with $45Ca^{2+}$ in the presence of 1mM $CaCl_2$. A representative autoradiogram (upper panel) and quantified signals (lower panel) are shown. A96, n=3 hearts; S96, n=3 hearts.